UNIVERSITÀ
POLITECNICA
DELLE MARCHE

DEPARTMENT OF ENGINEERING

Master's Degree in Biomedical Engineering

Finite Element Analysis Model to Study the Dynamics of Valgus Knee After Total Arthroplasty

Supervisor:

Prof. Marco Mandolini

Candidate:

Federica Pia Tarantino

Co-supervisors:

Prof. Lorenzo Scalise

Prof. Antonio Pompilio Gigante

Academic Year 2020-2021

I. Contents

II. List of figures

III. List of tables

Acronyms

TKA = total knee artrhoplasty

ROM = range of motion

OA = osteoarthritis

VD = valgus deformity

FEA = finite element analysis

ACL = anterior cruciate ligament

PCL = posterior cruciate ligament

MCL = medial collateral ligament

LCL= lateral collateral ligament

PTA=post-traumatic arthritis

RA = rheumatoid arthritis

Bi-UKA= bicompartimental total knee arthroplasty

UHMWPE = Ultra-High-Molecular Weight Polyethylene

CR = cruciate retaining

PS = posterior stabilizing

CKK = condylar constrained knee

FEM = finite element model

PFPS = patellofemoral pain syndrome

LPFL= lateral patellofemoral ligament

MPFL= medial patellofemoral ligament

FRPHE = fibrilreinforced porohyperelastic

PT = patellar tendon

QT= quadriceps tendon

MPTL= medial patellotibial ligament

Abstract

Total knee arthroplasty (TKA) is a successful procedure in the field of orthopedic surgery. Behind its application, there is its strict correlation to the most common form of arthritis: osteoarthritis (OA), an inflammatory condition that occurs when one or many joints undergo degenerative changes. Although TKA remains a reliable surgery in patients suffering from debilitating advanced degenerative arthritis knee, it has been reported that approximately 20% of patients are dissatisfied after the surgery. A possible reason for this discontent could be the presence of some deformities i.e., valgus deformity. The most common complaint after TKA is abnormal patellar tracking. Obtaining proper kinematics of the patellofemoral joint is difficult to study starting from in vitro analysis. Thus, since the complexity of knee kinematics has always challenged and fascinated the scientific community, the researchers have explored other tools to better understand the behavior of the knee. In this context, finite element analysis (FEA) has made its way. Even though the FEA has been largely applied in the field of orthopaedic surgery, some aspects remain untreated. Thus, the present work aims to apply the FEA in the case of valgus knee misalignment to assess which could be the pitfalls of the cruciate-retaining (CR)-TKA prosthesis and to obtain the kinematics pattern of the patellofemoral joint. The results obtained from the FEA are encouraging. Firstly, it has been pointed out an increase of the contact between the femoral component and patella with the rise of flexion angle. The analysis of von Mises stresses on the insert has revealed an abnormal distribution between the lateral and medial plateau at all flexion angles. The patellofemoral trends have been computed to assess the kinematics. From the reported findings it can be inferred that the finite element model employed in this work can study the dynamics of the postoperative valgus knee. This may be a step toward new research aimed at the development of TKA designs able to reduce the patient's dissatisfaction.

Riassunto

L'artroplastica totale del ginocchio (TKA) è una procedura di successo nel campo della chirurgia ortopedica. Dietro la sua applicazione c'è la sua stretta correlazione con la forma più comune di artrite: l'osteoartrosi (OA), una condizione infiammatoria che si manifesta quando una o più articolazioni subiscono alterazioni degenerative. Sebbene la TKA rimanga un intervento chirurgico affidabile nei pazienti affetti da artrite degenerativa avanzata del ginocchio debilitante, è stato riportato che circa il 20% dei pazienti è insoddisfatto dopo l'intervento chirurgico. Una possibile ragione di questo malcontento potrebbe essere la presenza di alcune deformità, ad esempio deformità in valgo. Il disturbo più comune dopo la TKA è il tracciamento rotuleo anormale. L'ottenimento di una corretta cinematica dell'articolazione femore-rotulea è difficile da studiare a partire dall'analisi in vitro. Pertanto, poiché la complessità della cinematica del ginocchio ha sempre sfidato e affascinato la comunità scientifica, i ricercatori hanno esplorato altri strumenti per comprendere meglio il comportamento del ginocchio. In questo contesto si è fatta strada l'analisi agli elementi finiti (FEA). Anche se la FEA è stata ampiamente applicata nel campo della chirurgia ortopedica, alcuni aspetti rimangono non trattati. Perciò il presente lavoro mira ad applicare la FEA nel caso di disallineamento del ginocchio in valgo per valutare quali potrebbero essere le insidie della protesi di ritenzione del crociato e per ottenere il pattern cinematico dell'articolazione femore-rotulea. I risultati ottenuti dalla FEA sono incoraggianti. In primo luogo, è stato evidenziato un aumento del contatto tra componente femorale e rotula con l'aumento dell'angolo di flessione. L'analisi delle sollecitazioni di von Mises sull'inserto ha rivelato una distribuzione anormale tra il piatto laterale e quello mediale a tutti gli angoli di flessione considerati. Le tendenze femore-rotulee sono state calcolate per valutare la cinematica. Dai risultati riportati si può dedurre che il modello agli elementi finiti impiegato in questo lavoro può studiare la dinamica del ginocchio valgo postoperatorio. Questo può essere un passo verso una nuova ricerca finalizzata a nuove protesi per ridurre l'insoddisfazione del paziente.

1 Introduction

The appearance of total knee arthroplasty (TKA) was a significant milestone in the history of orthopedic surgery [1]. The development of TKA began in the early 1970s when the first-ever procedure was completed. Since then, there have been efforts to guarantee an improvement of implant life, functionality for the patients and, instrumentation [2]. The success of the TKA procedure is related to its ability in relieving the pain of patients and restoring the function of the knee joint [3]. Approximately 700,000 TKAs are performed annually in the United States. The most common age group for total knee replacements remains from 65 to 84 years [4]. Projections suggest that the demand for TKA will rise by 673% by the year 2030 based on several factors: growth, aging, increasing the longevity of the population, obesity, younger age at implantation [2]. In the time between the first surgery and now, the close cooperation among surgeons and engineering has led to revising the old-fashioned techniques and introducing new ones that have shaped the surgical environment by adapting them to the various pathological disorders. Improvements in the past techniques and the discovery of new materials have greatly increased their effectiveness, making TKA one of the most successful procedures in the field of orthopaedic surgery (**Fig.1**).

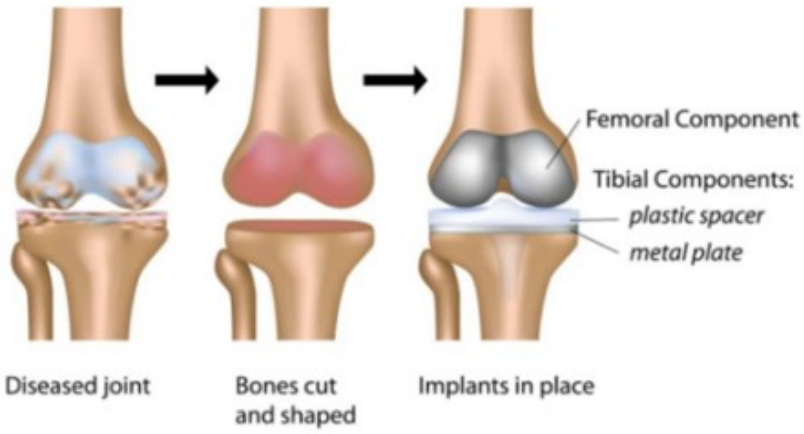

Figure 1. Illustration of TKA procedure.

TKA procedure involves the reconstruction of damaged joints accomplished through the resection of abnormal articular surfaces of the knee and their substitution using metal and polyethylene components [4]. Over time, design evolution in TKA had to satisfy these new needs: adequate range of motion (ROM) and control of the joint, long-term performance and fixation, transfer the load across the joint to bony structures, less material wear, better resistance to the stress, the weight, cost reduction, and anatomic congruence [5]. The main goal to perceive during the design and realization of a prosthesis is to guarantee the highest survival rate to avoid as much as possible revision surgeries [6]. Nowadays the survival rate of a knee prosthesis is about 90-95% after 10-15 years from the implantation; this is a very successful result but could become an issue in the case of the younger population which requires a survival rate of more than 15 years [7]. Behind the application of TKA, there is its strict correlation to the most common form of arthritis: osteoarthritis (OA), an inflammatory condition that occurs when one or many joints undergo degenerative changes, including subchondral bony sclerosis, loss of articular cartilage, and proliferation of bone spurs (osteophytes) [6]. OA occurs when the cartilage between joints breaks down or degenerates causing pain, loss of joint function, stiffness affecting a good quality of life. Although TKA remains a reliable surgery in patients suffering from debilitating advanced degenerative arthritis knee, it has been reported that approximately 20% of patients are dissatisfied after the surgery [8]. A possible reason for this discontent could be the presence of some deformities. Indeed, it has been estimated that 10% to 15% of the patients requiring a TKA are affected by valgus deformity (VD) i.e., tibiofemoral angle of greater than 10°. Typically, VD is the result of changes to both the soft tissues and bones around the knee. According to the literature, OA is the most common cause of VD [9]. In fact, it has been reported that OA can alter knee kinematics and stresses leading to abnormal kinematics motion. These kinematic changes alter the distribution of stress on the articulating surface. Until now, the relationship between cartilage loss in OA and kinematics is unclear [10]. The performance of TKA under this condition is still a great challenge to orthopaedic surgeons since after correcting the deformity, the achievement of knee stability is

strictly correlated to the work on the soft tissues which are altered around the knee joint [11]. Although several works have suggested TKA as a potential treatment for the knee with severe deformity, none has comprehensively reviewed the kinematic and anatomic variables which must be considered to achieve a good performance. Consequently, challenges posed by correcting VD and by considering OA have led the authors to examine the more frequent postoperative complications which may impair the outcome of TKA. Among the possible complaints after the TKA procedure, patellofemoral complications are the most common cause of complaints after TKA. The patella, indeed, acts as leverage to the muscular force generated by the quadriceps and its wrong placement could compromise the long-term success of the intervention. Obtaining proper kinematics of the patellofemoral joint is crucial to achieve a good postoperative clinical outcome [12]. Specifically, the study of the trochlear morphology has fundamental importance since major problems that occur after knee prosthesis implantation are attributed in part to an unnatural sulcus geometry i.e., high/low patella or excessive medial-lateral (ML) translation [12]. Thus, the knowledge of the patellofemoral joint is indispensable to determine the difference between a healthy or pathological knee and to understand the causes of patient dissatisfaction after the procedure. In this scenario, the finite element analysis (FEA), has made its way allowing a detailed analysis of the joint behaviour. FEA is considered a useful tool to predict strain and stress in complicated systems in bioengineering and biomechanics [13]. However, several assumptions such as lack of articular cartilage and other connective tissue have usually been made to simplify the knee behaviour making the knee model less realistic [14]. Since the accuracy in FE model predictions depends directly on assumptions made in the model, an anatomically accurate design could increase the possibility to obtain a more realistic simulation of the complex knee joint biomechanics. Indeed, FEA has long been recognized as a reliable tool to investigate the biomechanical behaviour of healthy knees. Additionally, it can be used to assess the eventual onset of some pathologies, like OA, and consequently understand if the performance of the TKA is required. Despite TKA has revolutionized the care of patients with end-stage knee arthritis, its goal of relieving pain and re-establish knee

function in a substantial proportion of patients is not achieved until now. Furthermore, even if the FEA has been largely applied in the study of the human knee kinematics, its implementation for the exploration of postoperative patellofemoral joint continues to be still little applied. Considering this, the present work aims to develop a 3D finite element knee model to study the dynamics of the valgus knee after the TKA performance.

1.1 The human knee joint

The knee joint is a complex structure in the body that undergoes critical loading while performing several daily life activities such as walking, jumping, running, sitting [15]. It serves as the junction for the movements of human lower extremities since it allows the rotation, twist, and slide of the femur relative to the tibia. Given the complicated anatomical structure and the variety of movement patterns of the knee joint, it is necessary to describe in detail its anatomy and its biomechanics. Indeed, the study of human joint behaviour is one of the challenging research fields that have witnessed significant developments over the last years [16].

1.1.1 Anatomy

The human knee is a synovial hinge joint and the largest joint in the body. The knee allows locomotion with the minimum energy requirements from the muscles and provides stability during several daily life activities [17]. The normal function of the knee requires an accurate balance between stability and mobility that depends on the interplay of several anatomical structures: bony structures, ligaments, joint capsules, muscles, and tendons [18]. The knee consists of bony articulations: the articulation between the femur and tibia supports most of the body weight, while the articulation between the patella and femur creates a frictionless transfer of the forces generated after the contraction of the quadriceps femoris muscle [19].

1.1.1.1 Bone architecture

The knee joint is composed of four bones: the femur (thigh bone), tibia (shin bone), fibula (calf bone), and patella (kneecap) (**Fig. 2**).

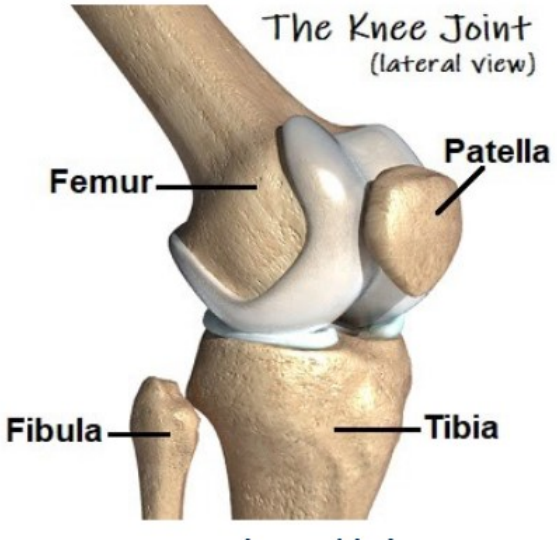

Figure 2. Lateral view of the knee joint.

The femur is the longest and strongest bone in the human body. The proximal epiphysis is a hemispherical head that articulates with the acetabulum in the pelvic bone forming the hip joint. While the distal femoral epiphysis forms a double condyle, lateral and medial, which makes up the knee joint together with the proximal extremity of the tibia. The femoral condyles are two oblong and convex prominences that are separated by a groove, where the patella is located; inferiorly they are separated by a deep notch called the intercondyloid fossa while anteriorly, they are flattened and expanded [20]. The shape of these condyles plays a fundamental role in the movement of the tibia on the femur. Specifically, the condyles act approximately as two rolling spheres, allowing the interaction with the tibia along the flexion-extension axis. Condyles present an asymmetrical geometry: in fact, the medial condyle is elliptically flatted, more massive, and less prominent than the medial one. In contrast, the lateral condyle is ball-shaped, wider, shorter, and is positioned more sagittal than the medial one. In addition, the lateral condyle transmits more weight to the tibia since it is more directly in line with the femoral shaft.

In contrast, the medial condyle is narrow crosswise and due to its longer rolling surface, it provides a major articular area [21]. The condyles have the radius of curvature that decreases going from the anterior to the posterior area influencing the behaviour of the femur during the motion of the knee. The line which connects the ends of all the radiuses creates a J-curve (**Fig. 3**).

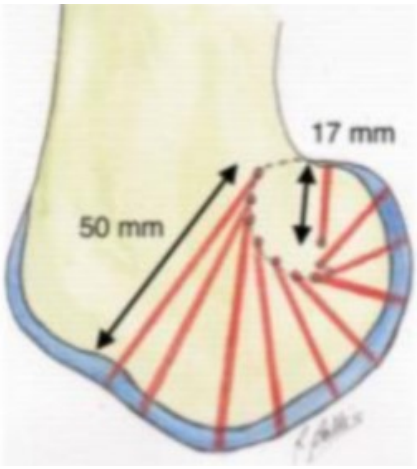

Figure 3. J-curve of the femoral condyles.

Special curving of the femoral condyles is important for the knee mechanics and can affect the stabilizing of the knee under compressive loads [21]. Anteriorly, the condyles are separated by a depression: the femoral trochlea. The two condyles are connected anteriorly by a smooth depression, the patellar groove over which the patella glides back and forth during knee flexion and extension. They are separated posteriorly by a deep non-articulating groove, the intercondylar notch. The patellar groove surface extends downward to the intercondylar notch, and it is made up of two slopes. The tibia is a long bone, exceeded only by the femur. It is subdivided into three major portions: the proximal end (also called the proximal epiphysis), the body (or shaft), and the distal end (also known as the distal epiphysis). The tibia is composed of two asymmetric plateaus, medial and lateral. The lateral tibial plateau is smaller and more rounded. While the medial tibial plateau is larger and more oval [22]. A peculiarity of the tibial plateau is its posterior slope (with the anterior elevation being higher than the posterior elevation); when this feature is considered in association with a large compressive joint reaction force, the force may have an anteriorly directed shear

component that acts to produce a corresponding anteriorly directed translation of the tibia [23] (**Fig.4**).

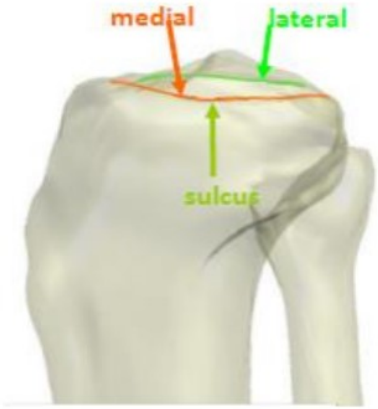

Figure 4. Tibial plateau.

The word patella means "little plate" in Latin. The triangularly shaped patella with its base facing proximally, apex facing distally, and two surfaces (anterior and posterior) is the largest sesamoid bone in the human body. The patella is asymmetrical, slightly wider than high, with an apex pointing distally that sits on the femoral trochlea. The patella does not fit perfectly with the femoral trochlea because the contact points between the femur and the patella vary with knee flexion. Specifically, at 20° of flexion, the distal pole of the patella contacts the femoral trochlea [24]. It rides in the tendon of the quadriceps femoris, the largest muscle of the thigh and the primary extensor of the knee. The dimensions of the patella are between 47 to 58 mm in length, 51 to 57 mm in width, and 20 to 30 mm in thickness and it has the thickest articular cartilage in the body. The patella is located anterior to the distal femur in the intercondylar notch between the quadriceps femoris muscle and the patella tendon. The patella's role is to transmit the forces of the extensor mechanism and to increase the area of contact between the patellar ligament and the femur. It articulates with the femoral trochlea forming the patellofemoral compartment and it also increases the moment arm of the quadriceps mechanism. The patella increases extension force as much as 50% (**Fig. 5**).

Figure 5. Triangularly shaped patella.

The fibula is a thin bone in the lower leg and runs along the lateral side of the tibia. It articulates with the tibial head and the ankle joint. The fibula is connected to the tibia via the interosseous membrane. The fibula does not articulate with the femur or patella. Furthermore, the fibula is not directly involved in weight transmission. Its main function is to combine with the tibia and provide stability to the ankle joint.

1.1.1.2 The cartilage

Articular cartilage (or hyaline cartilage) is a thin and elastic kind of tissue in the knee joint that covers the posterior surface of the patella, the tibial plateaus, the femoral condyles, and the patellar groove. It is a tissue without vascularization and innervation, therefore when it gets damaged, it is not possible to detect it until a bone rubs against another bone. The thickness varies depending on the joints. The knee cartilage is very thick: 6–7 mm at the patellofemoral joint, 5–6 mm at the femorotibial compartment. The main roles of the cartilage are to increase the area of contact of the articular surfaces to obtain a more homogeneous distribution of the forces on the bones; allow relative motion of the bone involved with minimal friction; reduce the load that occurs at the articular surface, acts as a shock absorber. Two types of cartilage are present in the knee: the hyaline one, covering the surface along which the joints

move, and the fibrous one, which mainly composes the menisci. Cartilage is subjected to wear over the years and has a very limited capacity for self-restoration (**Fig.6**).

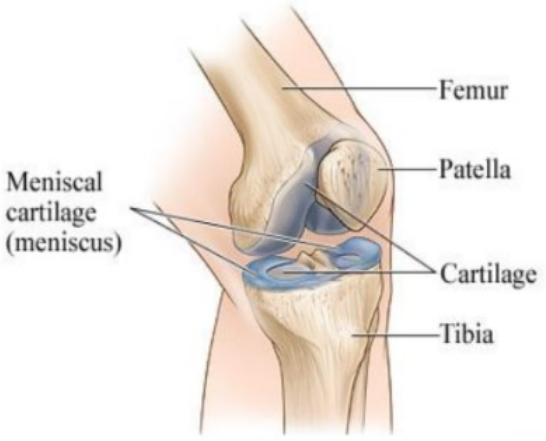

Figure 6. Cartilaginous structures in the knee.

1.1.2 Soft tissues

The bone structures of the knee are fully constrained by soft tissues: the menisci, the ligaments, the capsule, and the quadriceps muscle group.

1.1.2.1 Menisci

The menisci are two crescent-shaped fibrocartilaginous structures (medial and lateral) accepting the convex femoral condyle superiorly and the peripheral tibial plateau inferiorly. They are responsible for multiple actions: the improvement of joint congruence between the femoral condyles and tibial plateaus, the transmission of loads by increasing the contact area, and the proprioception of the knee joint. Without them, the nonconformity between the femoral condyles and tibial plateaus would lead to increased contact stress during motion and consequently would cause the onset of the complications [20]. They consist of connective tissues with collagen fibers containing fibroblast and fibrocartilaginous cells. Collagen fibers are mainly arranged circumferentially, crossed by radial fibers, improving meniscal strength and rigidity. Only the peripheral third of the meniscus is vascularized; the central portion remains

avascular. The peripheral section is thick, convex, and adherent to the joint capsule, while the central part is thin and unconstrained to the joint. The blood supply of the medial and lateral menisci differs between the two sections. In fact, the medial meniscus receives a greater blood supply than the lateral one and consequently, injuries involving the lateral meniscus require longer rehabilitation. In addition, the lateral menisci are much more mobile than the medial ones [20]. The menisci are made of three segments: anterior horn, posterior horn, and body. At the lateral meniscus, the horns have the same sizes, while at the medial meniscus, the posterior horn is larger than the anterior horn. The medial meniscus is generally semi-circular, larger, and thicker than the lateral and measures approximately 3.5 cm. It matches the medial tibial plateau's shape. The lateral meniscus is almost circular and covers a larger portion of the lateral tibial plateau. It is much more mobile than the medial meniscus with the ability to move 1 cm anteroposterior and laterally (**Fig.7**).

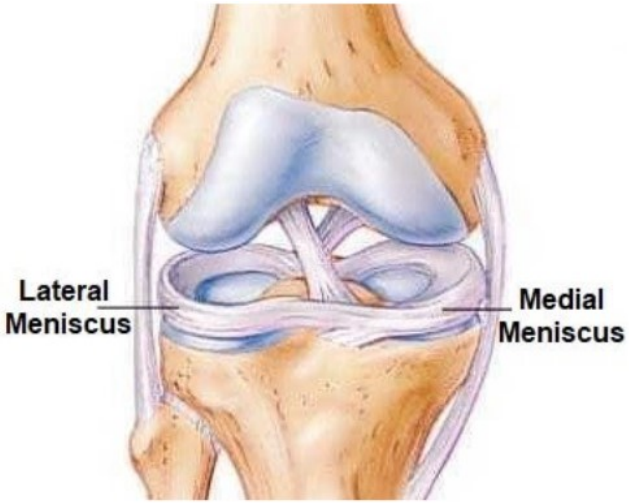

Figure 7. Lateral and medial menisci.

1.1.2.2 Ligament

The knee is stabilized by both primary and secondary stabilizers. Primary knee stabilization is achieved through knee ligaments, while muscles represent the secondary stabilizer [20]. Ligaments consist of closely packed collagen fiber bundles that provide support to the joint articulation and prevent excessive movements [24].

The major ligaments of the knee joint are:

- cruciate ligaments;
- collateral ligaments.

The cruciate ligaments are localized within the capsule and are surrounded by a synovial layer. They connect the femur and the tibia and in doing so, they cross each other obliquely, hence the term 'cruciate'. They are divided according to their site of attachment to the tibia into the anterior cruciate ligament (ACL) and posterior cruciate ligament (PCL). The ACL arises from the anterior part of the intercondylar eminence of the tibia and extends to the posterolateral aspect of the intercondylar fossa of the femur. It consists of two bundles, a posterolateral (PL) and an anteromedial (AM) bundle. The PL bundle is an important limitation to rotational moments of the knee, while the AM bundle is a restraint to anterior-posterior translation of the knee. During passive flexion, the AM bundle is tauter, while during passive extension movement, the PM bundle is tauter. The principal role of ACL is to limit excessive anterior translation of the tibia and excessive posterior translation of the femur. The ACL is considered the main stabilizer of the knee since it contributes to about 85% of the knee stabilization and allows smooth and steady flexion and rotation of the knee. The PCL rises from the posterior part of the intercondylar eminence of the tibia and moves to the anterolateral aspect of the intercondylar fossa of the femur. Its main function is to withstand an excessive anterior femoral translation or an excessive posterior tibial translation. As ACL, the PCL is composed of two bundles, the posteromedial (PM) bundle and the anterolateral (AL) [25]. The collateral ligaments ensure joint stability in the mediolateral direction and prevent undesired motion. They include the medial collateral ligament (MCL) and the lateral collateral ligament (LCL). MCL stabilizes the medial surfaces of the knee, minimizing the valgus and internal rotation during flexion; LCL runs from the femur to the fibula to stabilize the lateral surface of the distal femur to the proximal fibula preventing excessive varus stress and external rotation at all positions of knee flexion [25] (**Fig. 8**).

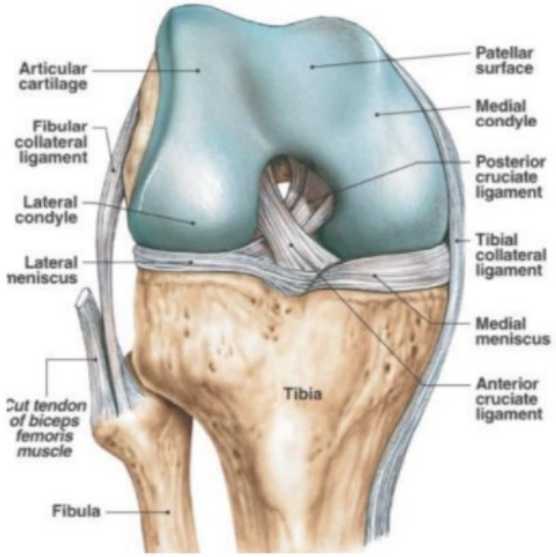

Figure 8. Knee ligaments.

1.1.2.3 Synovial capsule

The articular capsule is a fibrous membrane of varying thickness placed around the knee joint. It inserts on the peripheral part of the patella and the lateral edges of the patellar tendon. Distally, it is inserted around the edge of the tibial plateau and on the periphery of the menisci. Medially, the articular capsule is placed on the peripheral surface of the femoral condyles. Proximally, it inserts to the anterior surface of the cortex of the femur. It joins the base of the patella on the deep surface of the quadriceps [25]. The deep surface of the capsule is covered by the synovial membrane that is composed of synovial fluid functioning as a biological lubricant for the joint, absorbing shocks, allowing the sliding and rotation of the tibial cartilage with respect to the femoral cartilage, and providing low-friction and low-wear properties.

1.1.2.4 Muscles

The secondary stabilizers of the knee joint are all the muscles. The primary function of muscles is to produce the motion of the knee but also interact with the neuromuscular system to control knee motion [20]. Specifically, the stabilization and the movement of the knee in flexion and extension are guaranteed by two main muscle groups in the leg i.e., the hamstring muscles and quadriceps muscle. The hamstring

muscles consist of three muscles: semitendinosus, semimembranosus, and biceps femoris muscle. These muscles run along the back part of the femur and attach to the fibula and tibia to flex the knee. Conversely, the quadriceps muscle consists of four muscles: rectus femoris, vastus lateralis, vastus medialis, and vastus intermedius. These muscles attach to the proximal part of the tibia through the quadriceps tendon and through the patellar tendon inserts to the tibia (**Fig. 9**).

Figure 9. Anterior view of quadriceps.

The quadriceps produce a force that not only permits the extending moment in the knee but also guarantee together with the patellar tendon, that the patella is kept in the trochlear groove of the femur [26] The hamstring muscles are biceps femoris, semitendinosus and semimembranosus as shown in **Fig. 10**.

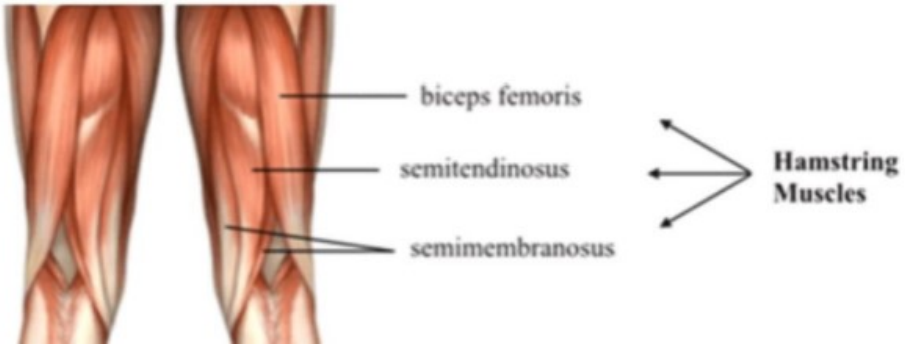

Figure 10. Posterior view of hamstrings muscles.

1.1.2.5 The tendons

Tendons are structures that join muscle and bone and transmit the forces produced by muscles to bones allowing the movement of the knee joint. In particular, the quadriceps act to extend the knee through the quadriceps patellar tendon mechanism indeed the quadriceps tendon fibers extend across the anterior surface of the patella and blend distally with the patellar tendon. This last one is considered one of the strongest collagenous structures of the body and it is designed for the transmission of high tensile loads and to keep the patella close to a constant distance from the tibia. In addition, the medial and lateral hamstrings act to flex the knee through their respective tendons. Furthermore, the iliotibial band performs a counterbalanced activity to the knee adduction moment, ensuring lateral stabilization [20].

1.2 Patello-femoral joint movement

The inferior part of the femur presents a pulley-like structure called the femoral trochlea. It is like a fixed pulley, and it is made up of medial and lateral faces, one inclined with respect to the other, that delimit the trochlear sulcus. The principal goal of the trochlear sulcus is to stabilize the kneecap allowing its sliding movement during the flexion-extension action of the lower limb. The function of the patella is multifaceted. Its primary goal is to serve as a mechanical pulley for the quadriceps as the patella changes the direction of the extension force throughout knee ROM. Its contribution directly increases with progressive extension. In addition, the patella works as a bony shield for the anterior trochlea and since it is interposed between the quadriceps tendon and femur it prevents excessive friction between the femoral condyles and the quadriceps tendon. The movement of the patella relative to the femur or femoral groove during knee flexion-extension is defined as patellar tracking. In the TKA procedure, the correct patellar tracking is important to optimize the position of the patella for extensor efficiency whilst maintaining a stable tibiofemoral joint. In most primary TKAs the achievement of the patellar tracking is linked to the correct

implant of the femoral and tibial components [26]. Since the patella travels only a small distance along the femoral trochlea, it should be a straightforward task to measure and comprehend the patellar kinematics. To understand the patellar kinematics, the motion of the patella relative to the femur must be considered: it is described in terms of 6 degrees of freedom (DOF), three translations, and three rotations. In clinical terms, these movements have been described as medial/lateral shift, proximal/distal translation, anterior/posterior translations, flexion/extension, medial/lateral tilt, and medial/lateral rotation (**Fig. 11**).

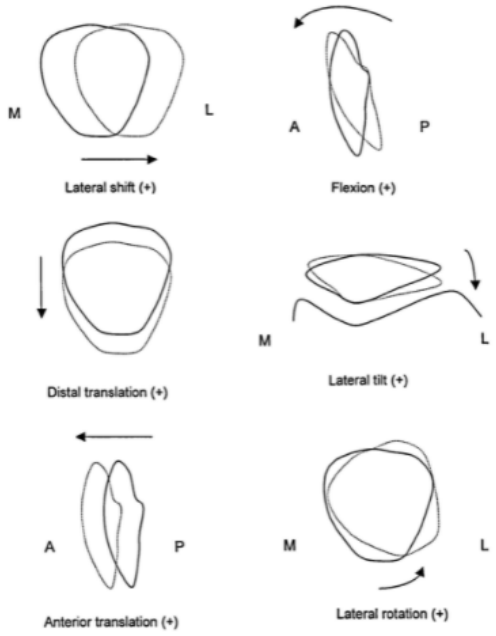

Figure 11. Definition of patellar motion.

1.2.1 Static alignment of the patella

The static alignment of the patella is correlated to the depth of the femoral sulcus, the shape of the patella, and the height of the femoral condyle wall. During the knee full extension in the frontal plane, the patella typically sits midway between the two condyles. In this configuration, the patella is superior to the trochlea and since the contact between the patella and femur is minimal, the patella is most mobile. While the same movement performed in the sagittal plane reveals that the apex of the patella rests just at or slightly proximal to the joint line. A way to measure sagittal plane

patellar position is the Insall-Salvati ratio, i.e., the ratio between the patellar tendon length and patellar height with the knee bent to around 30°. A ratio of 1.0 is considered normal; a ratio less than 0.80 indicates a "patellar Baja" which may be due to a shortened patellar tendon, while a ratio greater than 1.2 is called "patella Alta". In this last position, the patella takes longer to reach the bony constraint of the femoral trochlea, and consequently, the patella is at a greater risk of subluxation (**Fig. 12**).

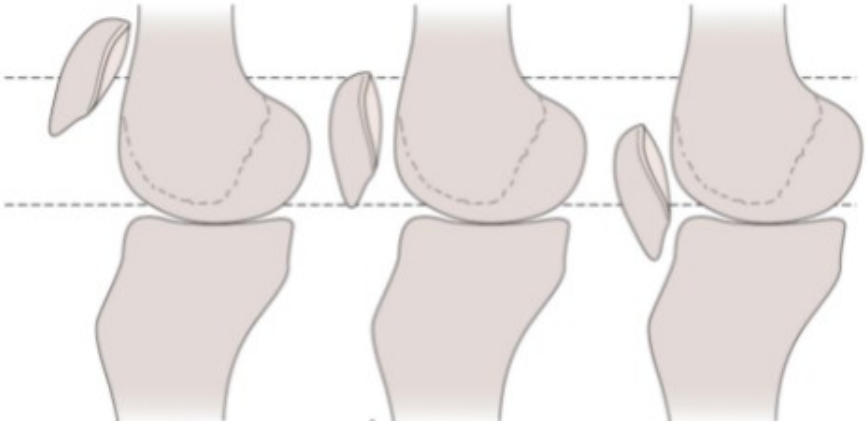

Figure 12. Patellar reference position.

1.2.2 Dynamic movement of the patella

The dynamic movement of the patella commonly referred to as patellar tracking is more important than the static alignment. The patella is a gliding joint and thus it has a movement in multiple planes. These movements are superior/inferior glide, medial and lateral glide, medial and lateral tilt, and medial and lateral rotation. Superior glide or patellar extension occurs when the quadriceps contract creating a superior pull on the patella. Inferior glide or also termed patellar flexion happens in conjunction with tibiofemoral flexion. Lateral and medial glides occur as translations in the frontal plane. The assessment of the dynamic movement can be done considering two typologies of chains: open chain and closed chain. During open chain motion the patella follows the path of the tibia, specifically, it glides inferiorly with knee flexion and superiorly with knee extension [12] (**Fig. 13**).

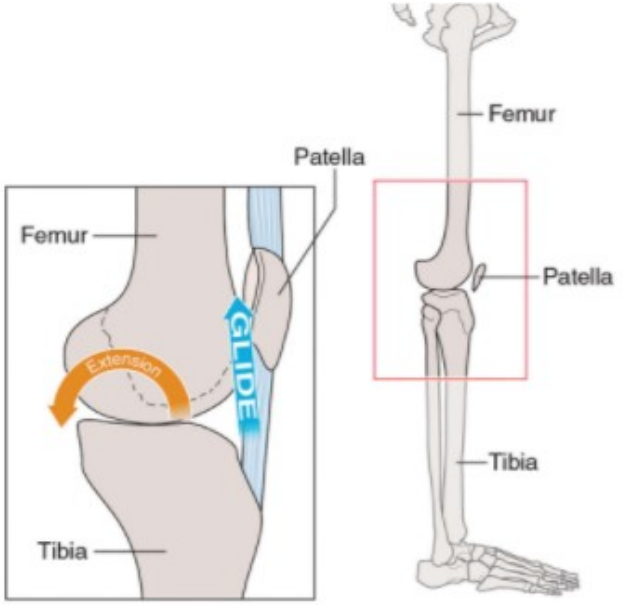

Figure 13. Open chain patellar motion with knee extension and knee flexion.

As the knee increases the flexion movement, the overall pattern of the patellar contact area increases, and this contact begins between the lateral femoral condyle and the lateral facet of the patella, at 30° degrees the contact is evenly distributed on both sides of the condyles. Then, at 60° degree of knee flexion, the superior half of the patella is in contact with the femoral groove slightly inferior to the contact area. At 90° degree, this contact area continues to increase and at this point, the superior portion of the patella is contacting an area of the femoral groove seated just above the notch. In deep flexion, the patella bridges the span of the intercondylar notch and during the full flexion, the odd facet is the only contact between the lateral surface of the medial femoral condyle and the patella. It is important to know that, in full extension, the patella moves slightly lateral due to the external rotation of the tibia [12]. Conversely, in closed kinetic chain movements, the patella is tethered within the quadriceps tendon so when the femur rotates in the transverse plane, it is the femoral surface that glides behind the patella.

2 Total knee prosthesis

2.1 Arthritis

The articular surfaces of the femur, tibia, and patella, which articulates with the femoral trochlea, are covered by superficial layers of cartilage that allow the sliding and the rotation of one component to the other with low friction. When the articular cartilage becomes damaged, arthritis, an inflammatory disease, occurs limiting joint mobility. Three types of arthritis affect the knee joints: OA, rheumatoid arthritis (RA), and post-traumatic arthritis (PTA). OA, the most common type of arthritis, occurs when one or many joints undergo degenerative changes causing a partial or total loss of cartilage and proliferation of bone spurs (osteophytes). Progression of OA could also lead the cartilage to completely disappear provoking a contact of bone and their rubbing leads to bone wearing causing an alteration in shape. Consequently, the balance configuration is compromised since the knee is not able to stand the full body and therefore cedes under loading [5]. In this new configuration, the stress needs to be redistributed so on the side of the knee that is clinically misaligned, greater pressure will be exerted and on the opposite side, the ligaments will be stretched [27] (**Fig. 14**).

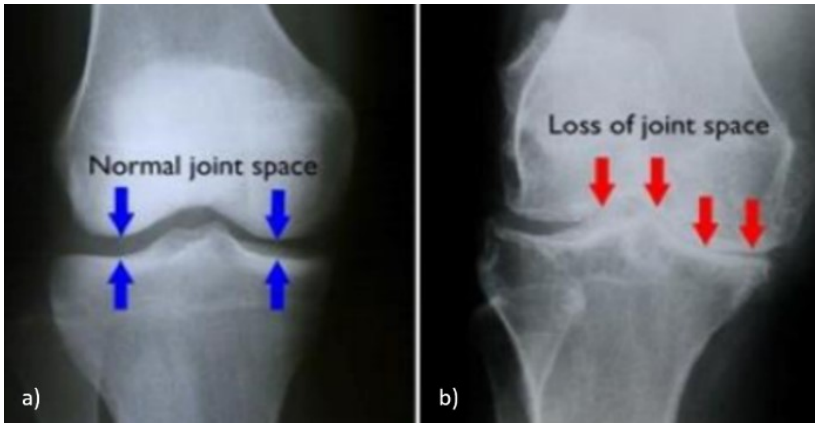

Figure 14. X-rays image of: a) healthy and b) arthritic knees.

RA is a chronic auto-immune disease in which the synovial membrane that covers the knee joint begins to swell causing knee pain and stiffness. It affects joints and internal organs. Symptoms of RA are different from those of OA. Joint stiffness lasts longer with RA, stiffness, and pain often occur in multiple joints and on both sides. The person may feel sick all over, lack energy, and his appetite. PTA can develop after an injury to the knee as fracture, soft tissue damage, meniscal tear. Its symptoms are like those of OA. Currently, the previously mentioned types of arthritis cannot be reversed, but symptoms can be effectively managed with lifestyle changes, physical therapies, and medications. But if they are not enough, surgery is required such as TKA. The next chapter explains in detail this procedure, its components, and the prosthetic implants present on the market.

2.2 TKA procedure

TKA is the most effective treatment for a total knee replacement for several advantages, such as relieving the pain of patients and restoring the function of the knee joint. Even a slight deviation in alignment in lower limbs can cause the loss of stability in the knee joint and an increase in the risk of wear-out failure and looseness rate of the implant. Thus, the restoration of lower body alignment is a key factor to achieve satisfying efficacy. The main goals of TKA are to restore the alignment of the knee, the ROM, the joint line, and the stability of the joint; to assure proper patellofemoral tracking, and to apply proper fixation techniques [3]. Preoperative planning is needed to determine the presence of any varus or valgus forces on the knee, by drawing the mechanical and anatomical axis on the X-Ray radiographs. Then the damaged joint surfaces are cut away and replaced with an artificial joint (prosthesis). The three prosthetic components are made of different materials: metal alloys, high-grade plastics, and polymers (**Fig. 15**).

Figure 15. TKA components.

The TKA is the most used procedure (90% of cases) in the case in which the OA affects both the medial and lateral articular surfaces of the knee joint and thus it is necessary to replace both. A drawback of TKA is the resection of bone stock and ligaments, resulting in an abnormal knee that could be especially disadvantageous for young and high demanding patients. Furthermore, to obtain a better fix of the tibial and femoral components of the prosthesis, stems are directly inserted into the bone itself. After 10-15 years from the first TKA, a revision is usually necessary to assess the proper knee alignment or remove the prosthesis and replace them with a second one characterized by longer stems. In the case of an isolated compartment OA of the knee, a well-accepted treatment is unicompartmental knee arthroplasty (UKA) [9]. In comparison with TKA, UKA allows for shorter operative times, less blood loss, minimal bone resection, smaller implants, and preservation of both cruciate ligaments. Since the UKA is going to replace only the knee compartment affected by OA, the cruciate ligaments are spared and thus the kinematics and proprioceptive activities of the native knee have been reported to be better preserved by UKA than by TKA (**Fig. 16**).

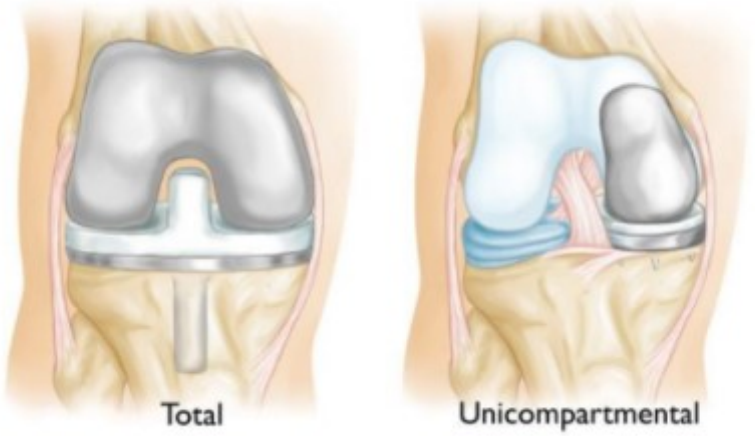

Figure 16. TKA components (on the left) and UKA components (on the right).

In addition to the previously described procedures, the Bi-unicompartmental knee arthroplasty (Bi-UKA) has been proposed to bridge the gap between UKA and TKA. It is performed when both the knee compartments, the medial and the lateral, are affected by OA. The Bi-UKA is so-called because, in contrast to the TKA, it consists of two UKA one for the lateral portion and one for the medial ones of the knee. Bi-Uni preserves the uninvolved compartment and the cruciate ligaments guaranteeing more physiological knee kinematics and improving proprioception. A careful selection of the patients must be done before performing this surgical procedure it is not recommended for obesity with varus in osteoporosis, inflammatory rheumatism, symptomatic patellofemoral arthritis flexural deformity greater than 10°, and severe combined laxity [29].

2.2.1 Surgical technique

On the day of surgery, the patient should be identified by the surgeon to confirm the correct side. The patient's preparation for TKA requires adequate muscle relaxation to facilitate the eversion of the patella and minimize tension in the quadriceps. Once the patient is prepped on the operating table, the skin incision can be made with the leg in extension or flexion. The cut starts 5-6 cm proximal to the tibia and ends on the medial border of the tibial tuberosity. In order to have access to the bones and remove the entire menisci, the patella and the medial patellofemoral ligament are moved

to the side and the ACL is removed. After that, the leg is placed a little bit more flexed to access the tibia and femur extremities. Firstly, the tibial plateau is cut strictly perpendicular to the long axis of the tibia; secondly, the posterior femoral condyle is cut, flexing the knee of 90° and drilling a hole in the femoral groove to have a reference point used to measure the size of the femoral component. A flexion gap is created by the cut of the tibial and posterior femoral condyle that can be measured by a spacer. The thickness of the spacer will correspond to the polyethylene insert of the knee prosthesis. In presence of valgus or varus forces, the spacer will be a spacer, and, in that case, a tibial recut or ligamentous release could be necessary. Indeed, a balanced flexion gap is required to obtain an adequate ROM and correct stability in the sagittal plane. Then, a condition of isometry of the collateral ligaments must be reached, and to do that the exact same rectangular flexion gap in the extension must be reproduced. So once the flexion and extension gaps are corrected, the chamfer and anterior femoral cut are performed. If necessary, the patellar cut is done being careful to not increase the thickness of the patella and the physiological structure with the implant; in fact, an over-cutting may weaken the patella and increase the risk of fracture, while on the other hand, a bigger thickness of the final patella may ruin the medial patellofemoral ligament by stretching it too much. Before implanting the prosthesis, a trial component is placed to check the complete ROM (**Fig. 17**).

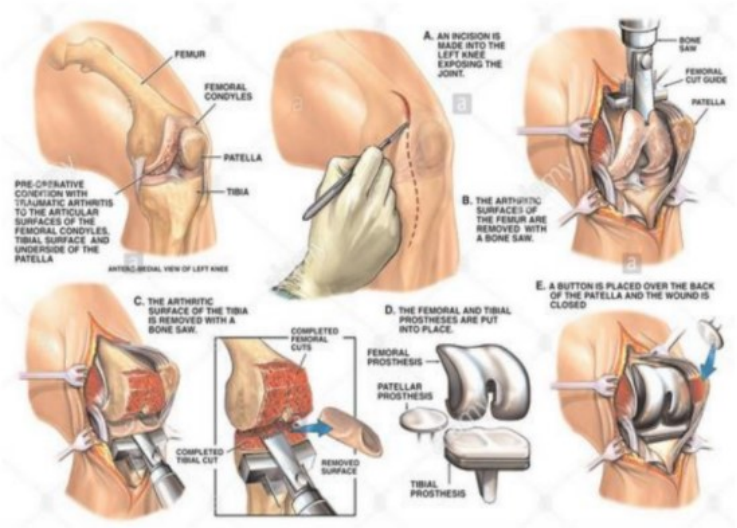

Figure 17. Steps of the TKA procedure.

Despite TKA being the gold standard procedure for the treatment of advanced knee arthritis, some studies have demonstrated that the long-term results in VD knee are relatively inferior to those of varus deformation. One of the main reasons may be the difficulty to acquire good soft tissue balance representing a challenge to the joint replacement surgeon. That's the reason the surgeon in the valgus knee should more confidently achieve soft tissue balancing to obtain a better load distribution and adequate stability [29].

2.3 TKA prosthetic components

The main needs that the design in TKA must satisfy are anatomic congruence, articularity, less material wear, and better resistance to the weight and to the stresses [2]. Generally, a total knee prosthesis is made of three parts: the femoral component, the tibial component, and the polyethylene insert (or spacer). In addition, if it is necessary the patella component could be considered and inserted. The femoral component is placed in the distal part of the femur and covers the lower end of the femur. The tibial plate is inserted into the center of the tibial bone and the third component is placed between femoral and tibial components.

2.3.1 Femoral component

The femoral component replaces the distal part of the femur. In many cases, the implants follow an asymmetric design to better reflect the asymmetrical geometry of the femoral condyles. Furthermore, since the patella during the knee flexion generates contact with the distal surface of the femoral component, asymmetric design is preferable to maintain the anatomical shape. To reduce the tension in flexion and to ensure a more physiological patella tracking also the condylar groove is asymmetric.
The condyles can be a single radius (SR) or a multiple radius (MR) design. SR design allows knee flexion and extension along a single axis benefiting the collaterals that maintain isometry and to the quadriceps that can generate a greater lever arm, whereas

the MR design is based on the J-shape of the native condyles. A correlation between the designs of the femoral component and the instability of the patella has emerged. Indeed, early designs of the femoral component have a shallow, flat trochlear groove that frequently induces an unstable patella. Normal knee function has been associated with the deep groove. The early hinged prosthesis has a narrow femoral flange, and it has a high rate of patellar subluxation and dislocation in the same way, the next generation of implants, also have either no groove or an insufficient groove for the patella inducing high patellofemoral stress. Nowadays, the designs are characterized by a smooth deep groove with a short, narrow notch that improves the patellar tracking and stability.

2.3.2 Polyethylene insert

The polyethylene insert is used to fill the gap between the distal femur and the proximal tibia created after the removal of menisci. The insert can be placed on the tibial component through a fixed or a mobile-bearing design. In the first case, pegs or matching shapes are used to attach it to the tibial plate; while in the second case it can rotate on it, minimizing the contact pressure. The polyethylene insert has an important role to create a smooth gliding surface and the role of z damper to absorb shocks and prevent luxation. Ultra-High Molecular Weight Polyethylene (UHMWPE) is usually used to construct the insert because it has excellent mechanical properties, such as elasticity, resistance to impact, abrasion, breaking, yielding, and fatigue, as well as low coefficients of friction, chemical inertness, and biocompatibility [30] (**Table 1)**.

Table 1. Mechanical features of UHMWPE.

Property	Value
Density	4.4 g/cm^3
Vickers hardness	30 MPa
Yield point	20 MPa
Young modulus	0.725-0.775 GPa
Elongation at break	300%

2.3.3 Patellar component

In some cases, the patella can also be replaced with a prosthesis. The patellar component improves extensor function by increasing its lever arm. There are different shapes of patellar components: cylindrical, convex, dome, and oval. A possible issue that may be present is the congruence with the femoral component groove.

2.3.4 Tibial component

The tibial plate is flat and has a stem that inserts into the center of the tibial bone. The tibial baseplate can be orthogonal or slightly inclined with respect to the stem. As for the polyethylene insert, also the tibial component can have a fixed or a mobile bearing. The fixed design has several drawbacks since it can be subjected to loosening, polyethylene wear, and transmission of extensive torque at the bone-implant interface thus the mobile-bearing design was introduced to improve the fixed on, and to allow high conformity bearing surfaces, a more natural motion, and reduce the stresses. The tibial component can be made up of titanium, satellite, or Ti6AI4V alloy.

2.4 Classification of TKA prosthetic implants

The classification of TKA prosthetic implants can be based on the replaced compartments, mechanical constraints, insert, and fixation method. The choice of the implant must be based on the degree of joint instability and the presence of bone defects. This section will be presented the classification according to the previously mentioned characteristics of the implants.

2.4.1 Classification based on the replaced compartments

Three types of implants are present in this category:

- Unicompartmental prosthesis: used when only one bone compartment is replaced. The ACL must be intact. It can be subdivided into tibiofemoral unicompartmental implants and patellofemoral implants. The first one consists

of femoral and tibial components that replace either the medial or lateral compartment. A unilateral metal femoral component substitutes the inferior and posterior surfaces of the native condyle, and a unilateral medial-tibial baseplate is inserted into the tibia; in the second one, the native trochlea is replaced by a metal trochlear component.

- Bicompartimental prosthesis: both the medial and lateral tibial and femoral components are substituted at the same time. The native patella is retained.
- Tricompartimental prosthesis: all tibiofemoral and patellofemoral compartments are replaced by a metal femoral component, a polyethylene insert, and polyethylene patella. If the patella is damaged, it is substituted by a metal backed.

2.4.2 Classification based on the mechanical constraint

Usually, the LCA is removed, while the LCP if it is intact is preserved. The part used to contrast the forces acting on the knee is called constrain. In this classification belongs the followed prosthesis:

- Cruciate retaining (CR) prosthesis: they preserve the PCL, not the ACL. The advantages of these are that they have the best longevity, more physiological biomechanics, more stability, and the possibility of fixation without cement as is shown in **Fig 18**.

Figure 18. CR prosthesis.

- Posterior-stabilising (PS) prosthesis: LCP is removed. They consist of thicker tibial inserts and present in the center, a ridge that articulates with a cam obtained in the femoral component and which together with this provides a brake to an excessive forward translation of the femur on the tibia avoiding the dislocation of the femur. PS prosthesis advantages: more possibility to obtain a more ligamentous balance, more predictable kinematics, and good flexion flexibility (**Fig. 19**).

Figure 19. PS prosthesis.

- Hinged prosthesis: They allow only flexion-extension movements in the sagittal plane. Their components both have long taps to be inserted into the medullary channels ensuring joint stability. They are used in case of extreme bone fragility (**Fig.20**).

Figure 20. Hinged prosthesis.

- Medial pivot prosthesis: This design has been created to reproduce the movement of the normal knee during flexion, called the "medial pivot". Specifically, it indicates the fact that during flexion there is a minimum movement of the medial femoral condyle and a posterior translation of lateral femoral condyle. It has been created with a medial condyle that has an identical curvature radius on the coronal and the sagittal plane and the lateral condyle is smaller than the medial with a cylindrical configuration to control rotation and to stabilize the knee. The medial pivot prosthesis design allows better ROM, better stability, longer polyethylene survival, and less wear stress on the tibial surface. An important key element of this design is the more reproducibility of the paradoxical motion, i.e., the problem in which the traditional models can't reproduce before the implantation, the roll-back mechanism but slide forward as it is shown in (**Fig 21**).

Figure 21. Medial pivot prosthesis.

2.4.3 Classification based on the insert

According to the movement between the insert and tibial plateau, two different models are distinguished:

- Fixed insert: The insert is fixed through a constraint to the tibial plate and is solid with its movement;

- Mobile insert: Rotational movements between the insert and tibial plate occur. They are designed to limit the polyethylene wear and the subsequent failure caused by osteocytes (**Fig.22**).

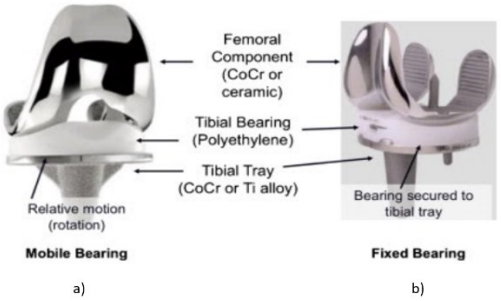

Figure 22. Two type of prosthesis: a) Mobile bearing prosthesis; b) fixed-bearing prosthesis.

2.4.4 Classification according to the fixation

There are two kinds of fixation for the prosthetic component: cement and cementless TKA implants. The first one is the most frequent prosthesis in which both the tibial and the femoral components are cemented with polymethyl methacrylate (PMMA). Cement makes the discontinuities uniform and acts as a damper being interposed between a material very rigid (the prosthesis) and a much less rigid one (the bone). Whereas the cementless prosthesis consists of a rough surface layer that ensures anchoring to the bone through a press-fit method. Among the typical problems related to cement use, there is wear since small fragments of resin can detach from the principal block [31] (**Fig. 23**).

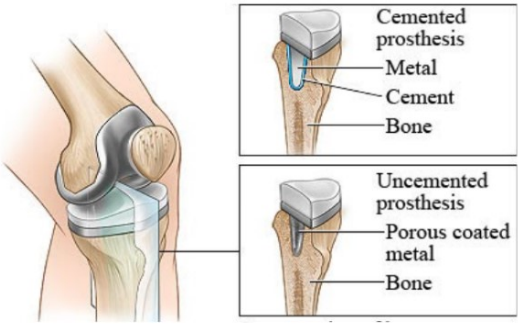

Figure 23. Cemented and uncemented prosthesis.

2.4.5 Implant choice in valgus knee

In the history of orthopaedic surgery, the correction of a knee joint VD has been considered a tough challenge. Despite the advances in these terrains, the type of ligament balancing approach and choice of appropriate implant represents an open debate still today due to a lack of scientific evidence-based studies. The implant selection should be carried out pre-operatively based on the radiological and clinical evaluation. In the case of frontal deformity in valgus, in patients with convex laxity and/or deformity surpassing 20°, achieving these two objectives may be difficult [9]. Specifically, the selection of the appropriate implant appears to be most relevant since the good, durable, and functional outcome of the TKA depends on this. Several TKA implant designs offer the surgeon options for individual patients. The different choices imply that each specific problem has a corresponding implant that provides a reliable solution. The principal goal of TKA is to attain optimum alignment, adequate balance, and deformity correction. Basically, the patients can receive either a fixed-bearing design or a mobile-bearing implant. Nowadays an overwhelming majority of TKR are "fixed bearing" divided into PCL preservation designs (CR) and PCL substitution designs (PS). Many works were carried out to evaluate which was the better design to ensure better results. Both guarantee reliability and duration during the years [2]. In the valgus knee, the PCL is often contracted, and this may limit the deformity correction. Moreover, it may be more difficult to obtain the deformity correction with an intact PCL because the PCL represents the secondary stabilizer. Furthermore, a PS

prosthesis has more stability than a CR one and allows for greater lateralization of the femoral and tibial components improving patellar tracking. So, since it has been suggested that it is simpler to substitute a contracted PCL with a PS design than to stabilize it with a CR one, some authors have recommended that a PS design can be used in VD (**Fig. 24**).

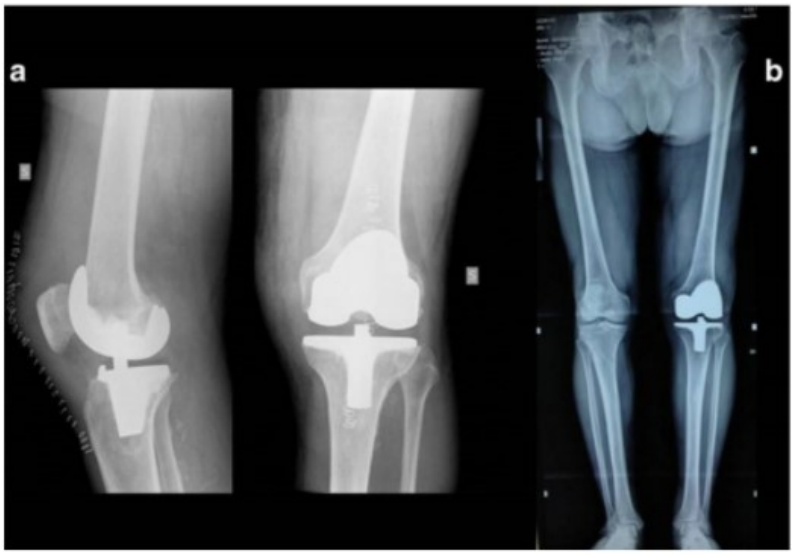

Figure 24. (a) Postoperative anterior-posterior and lateral views; (b) antero-posterior long lex view at 3 months showing a well-aligned left knee.

Other works have preferred CR design since the PCL retaining consents bone stock preservation with less fracture risk, permits an easier revision surgery, and guarantees extensor apparatus strength. The comparison of the femoral and tibial anatomic congruence has inferred that the CR congruence is less than PS one. it allows a greater ROM, but also causes prosthetic components instability due to sliding and wear stress increasing. PS design is inherently more stable than CR result so that it is applicable to most deformities and allows for greater localization of femoral and tibial components improving patellar tracking. Some prefer a PS implant since the surgeon must confidently achieve soft tissue balancing resulting in better load distribution and enhancing both longevity and component stability. The choice of implant, however, must be based on the degree of joint instability and the presence of bone defects so careful pre-operative planning is essential to estimate the grade of constraint that will be necessary. Indeed, for Grade I valgus knees, CR implants can be used but proper

bony resections are required for TKA long-term survival is mandatory to evaluate if it is present a fixed or a reducible VD: in the first case, after lateral soft tissue release, the knee may be unstable because both the medial and lateral structures will no longer be functional. Thus, in this case, the surgeon should also decide to implant a semi-constrained prosthesis, i.e., constrained condylar one. In case of laxity on the coronal

plane caused by an MCL insufficiency, PS, condylar constrained knee (CKK), or the hinged implant is preferred to achieve appropriate stability and deformity correction. In case of a mild coronal deformity (<10°) and inadequate MCL tension, a PS implant can be used. Whereas, in presence of more severe deformities many surgeons rely on a CCK implant since it has a larger cam and can adopt stems that dissipate joint stresses, with the drawback that is necessary to remove a larger portion of femoral intercondylar bone to accommodate the femoral box. Anderson et al. [33] have reported excellent results at a mean of 44.5 months follow-up in 55 primary CCK TKAs without stems for the treatment of valgus knee. Easley et al. [33] have carried out excellent clinical outcomes at a means of 7.8 years follow-up in the case of 44 consecutive primary stemmed CCK TKA without the presence of loosening, implant failure, flexion instability, or peroneal nerve dysfunction too. However, there are some drawbacks of CCK prosthesis as the polyethylene wear, the difficulty in revision TKA procedure after CCK prosthesis implantation, mechanical loosening due to load transfer, and periprosthetic failure. Rai et al. [33] have demonstrated that despite having a severe deformity and stiffness of the knee joint at a young age, primary CCK-TKA in post-traumatic arthritis provides satisfactory clinical outcomes with 94.7% prosthesis survival. Hence, they conclude that CCK-TKA is a good option for the treatment of post-traumatic arthritis of the knee but not without complications [9]. In the case of elderly patients with bone defects, VD greater than 20°, multiplanar instability, or rheumatoid arthritis, a hinged implant should be the solution preferably coupled with fixed bearing to improve patellar tracking in the valgus knee. Unfortunately, the hinged implants are subject to several limitations as the need to cement long stems into the tibia and femur hinder their removal during revisions and the risk of loosening or rupture of the implant. On the other hand, when the medial

soft tissue is no longer functional with certainty as in grade II, a higher constrained prosthesis is mandatory to obtain knee stability (**Fig. 25**).

Figure 25. Anteroposterior (on the left) and lateral (on the right) view showing the rotating hinge prosthesis implanted in a patient.

According to the literature, in patients with fixed deformity, constrained devices such as CCK and hinge types may achieve satisfactory results. Even if it is not so easy the selection the implant, it is possible to keep in mind the level of constraint that can be categorized as CR with minimal constraint, CS design, unlinked varus-valgus constraint, rotating hinge implant. The choice of the correct degree of constraint is based on the bone's condition and ligaments; if sufficient a primary PS design could be a good option; in case of insufficient collaterals, the ideal implant could be the semi-constrained design since it provides the minimum bone loss. Finally, in the case of severe ligament disruption and bone loss, the hinged prosthesis could be eventually chosen [62]. In [32] was demonstrated the therapeutic potential of mobile-bearing TKA in case of permanent patellar dislocation with tibiofemoral (TF) joint OA. In this case, an 80-year-old woman with permanent dislocation of the patella and severe VD has been considered and, it has been carried out that mobile-bearing TKA can theoretically adjust rotational malalignment by itself-align feature and improve patellar tracking and patellofemoral contact stress.

3 State of the art

Traditionally, the TKA procedure has been used as an effective treatment for OA, relieving pain and restoring knee function of the patients. However, a considerable number of patients are dissatisfied after the surgical treatment [33]. Anterior knee pain after TKA is one of the most common patient complaints that increases the revision rate. Several factors can induce persistent knee pain: prosthesis placement (excessive rotation, aseptic loosening), surgical procedures (ligament balance), infections. However, even when all these reasons have been ruled out, patients still describe anterior pain. The most important factors which affect this problem are surgical technique and prosthesis design. Several studies [34] have demonstrated the influence of femoral component modifications in the changes of patella tracking [35]. Among them, Meijerink et al. [36] have proved that the TKA medializes the trochlea producing an abnormal patellar tracking pattern which could result in patellar instability, pain, wear, and failure. Other authors [37] have focused on the difference between CR and PS design on patellofemoral contact pressure and kinematics demonstrating better results for PS TKA with respect to CR TKA inducing less frequent anterior knee pain. It has emphasized that the occurrence of patellar tracking is caused by rotational malalignment of the femoral and/or tibial components. Many investigations [38] have analysed the CR-TKA and CS-TKA on tibiofemoral kinematics, however, the influence of these kinds of prosthesis on patellofemoral kinematics is unclear. Thus, Keshmiri et al. have compared patellar kinematics in the natural and in the knee with a CR and CS-TKA demonstrating that there is no significant difference in patellofemoral kinematics between the two designs [39]. Planckaert et al. [40] have analysed knee 3D kinematics (flexion/extension, valgus/varus, and internal/external tibial rotation) of TKA patients with anterior knee pain and compare them to those of the asymptomatic TKA group, and a healthy control group. The study has revealed different gait kinematics

of painful TKA patients with respect to asymptomatic ones. Painful TKA patients presented three specific characteristics that tend to patellofemoral forces causing unexplained pain: a stiff knee gait, a valgus alignment when walking, and combined TKA components slightly internally rotated. Since the complexity of knee kinematics has always challenged and fascinated the scientific community, the researchers have explored other tools to better understand the behaviour of the knee. In this context, the FEA, also termed the finite element method (FEM), has made its way. FEA is a numerical process to solve engineering problems and mathematical physics. To solve the problem, it subdivides a large problem into smaller, simpler parts that are called finite elements. The simple equations that model these finite elements are then assembled into a larger system of equations to represent the entire problem. The main benefit of using FEA is that it is cost-effective, as running an analysis using this computational method is cheaper than performing a physical experiment. Modern finite element models are usually based on magnetic resonance imaging (MRI) and/or computed tomography (CT) scans and offer a high degree of anatomical realism. Specifically, FEA has been recognized significantly and widely used in the field of knee prosthesis to perform numerical simulations under different types of configurations and loadings; indeed, FEA is a useful tool for the prediction and measurement of local parameters such as internal stress, strain, and displacement or to detect abnormal forces generation which can be the cause of TKA failure and uncomfortable situations for the patient by affecting joint kinematics. An uncomfortable condition for a patient is knee misalignment which is considered one of the biomechanical key factors influencing the progression of knee OA. Valgus malalignment increases the risk of medial and lateral OA progression [27]. In this scenario, several works have applied FEM to both simulate different everyday life conditions and loads of normal knee joint or pathological one and to simulate possible complications in TKA to reduce the incidence of TKA revision and improve patient satisfaction after TKA. The studies obtained from accurate research in the literature have been divided into four different sections:

In Sec. 3.1 studies focused on the use of FEA to investigate the stresses and the

complications produced after TKA performance, and the patellofemoral joint biomechanics have been inserted.

In Sec. 3.2 all the works in which the FEA was applied to create a 3D model in the case of the valgus knee without the application of TKA have been grouped.

In Sec. 3.3 studies that have considered different assumptions to facilitate the ligaments representations in the FEA 3D models have been summarized.

In Sec. 3.4 works based on the study using FEA the patellofemoral joint kinematics before and after the TKA treatment.

3.1 FEA 3D models to study knee biomechanics

Ingrassa et al. (2013) [41] have applied the FEM to firstly compare two different PS knee joint prostheses (Stryker and Tornier) that were different mainly in the shape of the PE component and after the reshaping of the best solution, contact and equivalent stresses on the plastic insert of the two models have been calculated. The materials used for the prostheses were the Ti6Al4V and UHMWPE, due to their high biocompatibility and good tribological properties reported in **Table 2.**

Table 2. Material properties used in Ingrassa et al. Study [41].

Material	Young's modulus (MPa)	Poisson's ratio
Ti6AlV	110.000	0.34
UHMWPE	2.00	0.44

The CAD model of the prostheses has meshed into solid finite elements and different knee flexion angles configurations have been analysed. A load was applied along the femoral axis. FEM analyses have returned stress distribution at the interface between the femoral part and the plastic insert at 60°, 90°, and 120°, and in the stabilizing post-cam mechanism which is fundamental to prevent dislocations. Numerical comparisons have been performed in terms of contact and equivalent stresses on the plastic insert for both models. Furthermore, geometric modifications of the anti-

dislocation element have been proposed to enhance the stress distribution and minimize the risk of wearing and fracture damage. From these results, an optimization of the original prosthesis has been possible by reducing the stress peaks without affecting the kinematics of the joint. The two FEM models are shown in **Fig. 26.**

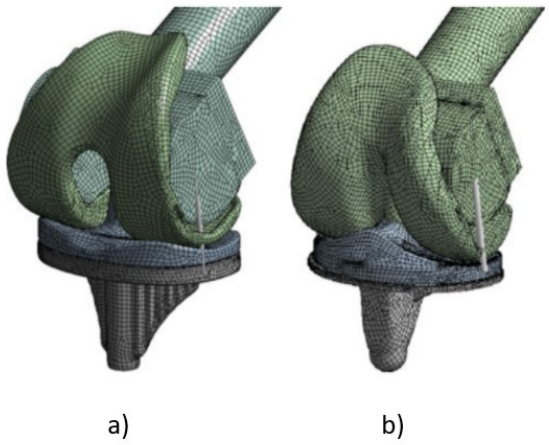

Figure 26. FEM models of the two prostheses. (a) Stryker model (B) Tornier model.

Islam et al. [42] have developed 3D FE models of the patellofemoral joint to quantify in vivo cartilage contact stress. The refined 3D model geometry was imported into Hyper Mesh to create the FE meshes of the femur, patella, patellar cartilage, and femoral cartilage (**Fig. 27**).

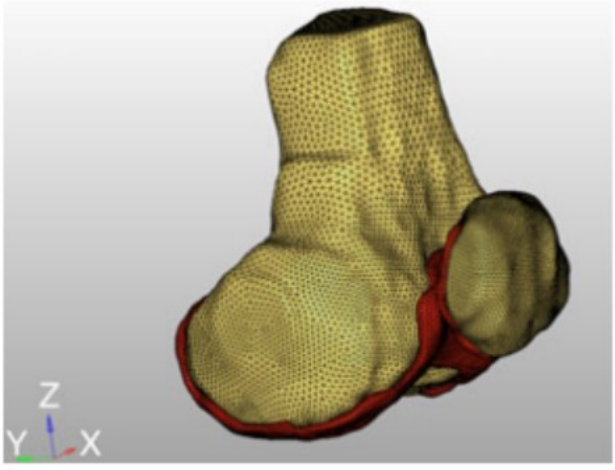

Figure 27. Finite element model of patellofemoral joint [42].

The patellar and femoral cartilages were modelled as a homogeneous isotropic material with a Young modulus of 12.0 MPa and a Poisson's ratio of 0.45. The femur and patella were modelled as linear elastic isotropic materials with a modulus of elasticity of 12.0 GPa and Poisson's ratio of 0.38. The bone structures, patella and femur have been considered rigid. Surface-to-surface contact was assumed based on the hard contact constraints and a very low coefficient of friction of 0.002 was assumed for the contact modelling. The femur was constrained in all six DOF at the proximal end for all simulations. All the four FE models were developed for the left knees of a healthy female subject and one pathological subject with patellofemoral pain syndrome (PFPS) at two different knee flexion angles. It has been demonstrated to have higher stress on the medial side of the patellofemoral joint for the pathological subject than the healthy subject leading to higher medial pain. Contact stresses, Von-Mises stress, and maximum principal stresses increase with the increasing of flexion angle. The FEA has shown higher stresses in the medial side of the PFPS subject (**Fig. 28**).

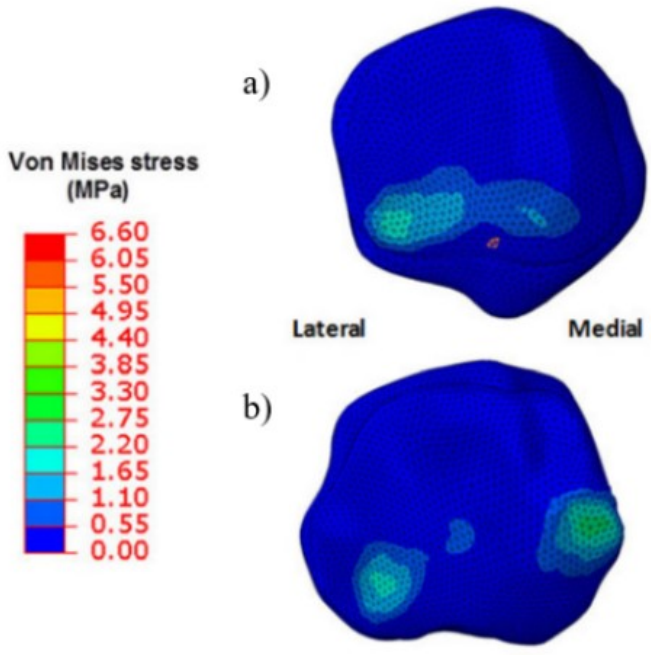

Figure 28. Patellar cartilage Von Mises stress for (a) healthy subject (max. stress of 2.1 MPa at lateral side); (b) PFPS knee (max. stress of 2.55 MPa at medial side) [42].

In [43], the development of a 3D solid biomechanical knee model consisting of femur, tibia, ligament, patella, cartilage, meniscus, and knee prosthesis has been proposed. In this regard, two total knee prostheses composed of the femoral implant, tibial implant, and polyethylene insert have been considered to reduce the stresses and strains in the tibia and tibial bone. Additionally, the nature of equivalent stresses with different biomaterials (elastomer and cement) has been investigated to find the best material for knee prostheses. The elastomer has been implanted between the tibia implant and the polyethylene insert in the four prostheses of the knee (Model (Ti6Al4V), Model II (CoCrMo), Model III (316L SS), Model IV (ZrO2)) and for model five of the knee prosthesis (Model V) attached the lower implant in the tibia bone with the cement. Solidworks 2016 has been implemented to solid modelling knee implant components. The FEA of the knee prosthesis instead has been performed in ANSYS workbench 16.2 by applying the load in the upper surface of the femur and fixed embedding at the low level of the tibia and tibial bone. Three models of the knee have been constructed: the first model is of an intact knee joint; the second one has been composed of the femoral implant, tibia implant, medial implant, polyethylene insert, elastomer and the third one has consisted of the femoral implant, tibial implant, polyethylene insert, and cement. These models have been created starting from bone structures and soft tissues taken from a healthy human knee of a 24-year-old man (**Fig. 29**).

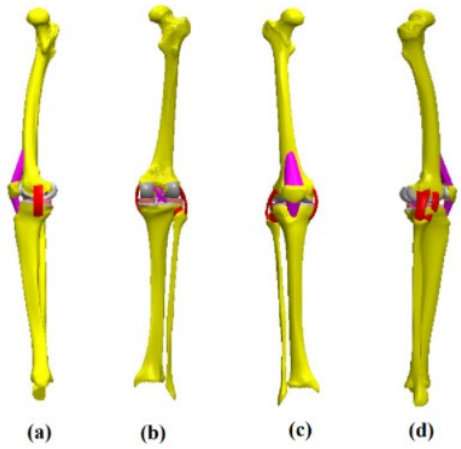

Figure 29. Different views of the knee model studied: (A)lateral view; (B) dorsal view; (C) front view; (D) lateral (right) view [43].

The material properties of the bone structures and prosthetic design used in this work are listed in **Table 3**.

Table 3. Material properties of different biocompatible materials used for prosthesis.

Material	Density (Kg/m^3)	Young's Modulus (MPa)	Poisson's ratio
Tibia	1.96	-	-
Femur	1.91	-	-
UHMWPE	930	690	0.29
Ti6Al4V	4430	115000	0.342
CoCrMo	8830	230000	0.3

The geometries have been modelled by tetrahedral elements, type Solid187. The resulting femur consisted of 479,497 elements and 676604 nodes; the tibia and tibial FE models of 447218 elements, 62440 elements, 625854 nodes, and 94168 nodes respectively; the patella consisted of 25094 elements and 36292 nodes. The femoral and tibial cartilage consisted of 57755 elements and 92406 nodes, the ligaments consisted of 41120 elements and 68096 nodes and finally, the menisci were composed of 10476 elements and 17312 nodes. The obtained FE model has been shown in **Fig.30**.

Figure 30. FE model of one of the three models obtained in this article [43].

The load and boundary conditions have been defined: the tibial tray and femoral component were fully bonded to the femur and tibia bone respectively. The PE mobile-bearing was free to make translation and rotation with respect to the surface of the tibial tray. A load of 500 N was applied to the upper surface of the femur which was constrained only in flexion-extension while the tibia and fibula were completely fixed at their distal ends as it is shown in **Fig. 31**.

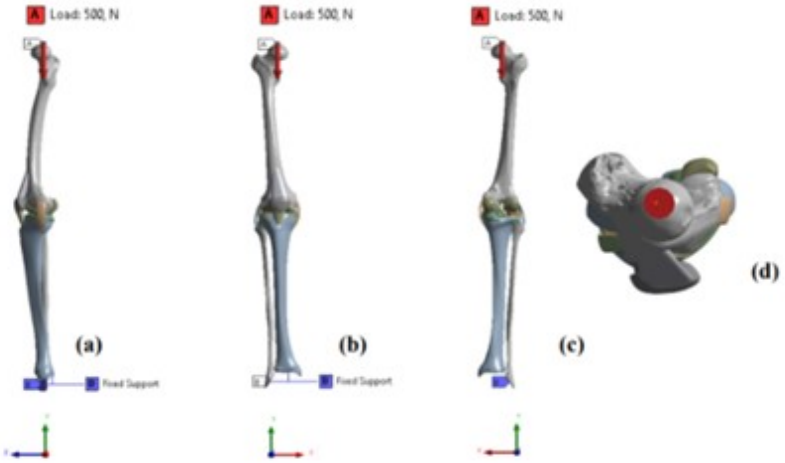

Figure 31. Boundary conditions in different views: (A) lateral (left) view; (B) front view; (C) dorsal view; (D) top view [43].

In 2019 [44], the patellar tendon release's effect on the movement of patellofemoral joint squat has been analysed to provide reference data for knee joint surgery. Starting from CT and MRI images of a healthy male volunteer, a 3D geometric knee model has been established. Then, a TKA prosthesis has been assembled **Fig.32**.

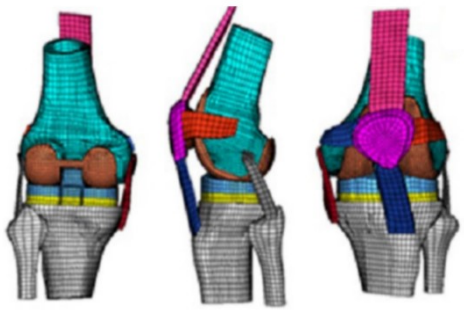

Figure 32. FEA model of the knee joint after TKA [44].

The simulation of patellar tendon release has been performed in Hypermesh software, version 11.0 (Altair Engineering Corp, MI, USA). A force of 400 N was applied to the quadriceps with a direction parallel to the femoral shaft. At the same time, half of the body's weight was applied to the center of the femoral head. Then, the reference point of the ankle was fully fixed with six degrees of freedom. The bone and femoral prosthesis have been defined as isotropic and linear elastic materials, respectively. The polymer polyethylene pad has been defined as non-linear elastic-plastic material. The soft tissue has been defined as nonlinear elastic. Between the polymer polyethylene and cobalt-chromium molybdenum material, a friction coefficient of 0.04 has been defined. Different flexion degrees have been simulated in ABAQUS software; version 6.10 (Dassault SIMULIA Corp., Paris, France). In a more recent study [45] FEA has been applied for the first time to investigate lateral patellofemoral stability in patients with symptomatic patellofemoral instability and dysplasia of the trochlear groove. MRI data of five healthy knees were segmented, meshed and an FEA has been performed. Then the force required to dislocate the patella by 10 mm and to fully dislocate the patella has been calculated in various knee flexion angles between 0° and 45°. Patellar kinematics were derived from the prescribed tibiofemoral kinematics in a static structural finite element (FE) simulation (ANSYS® Academic Research, 19.2). Ligaments have been modelled as tension-only springs. Specifically, the MPF ligament and lateral retinaculum have been modelled as four-tension-only springs with a total stiffness of 12 N/mm and 2 N/mm, respectively. Contact between the femur and the patella were modelled as frictional with a friction coefficient of 0.02. Bones were modelled as rigid structures with the femur fixed in space. Cartilage was treated as a rigid structure and deformation was considered by formulating contact behaviour with a penetration penalty (**Fig. 33**).

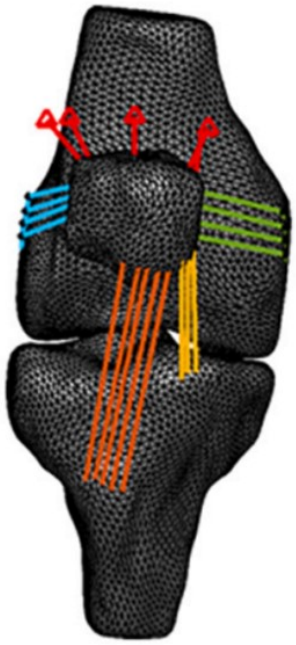

Figure 33. Illustration of the quadriceps muscle (red), MPFL (green), MPFL (yellow), lateral retinaculum (blue), and PT (orange) [45].

3.2 FEA 3D knee models in case of VD

Tarnita et al. [46]have applied the FEA to study the role of the articular cartilage in a complex 3D model of the healthy human knee joint, to develop the OA, and to simulate the biomechanical behavior of the knee joint. Three different cases for the valgus tilt of 10° have been developed which differ from each other by progressively increasing disorder areas in menisci, femoral and tibial cartilage (**Fig. 34**).

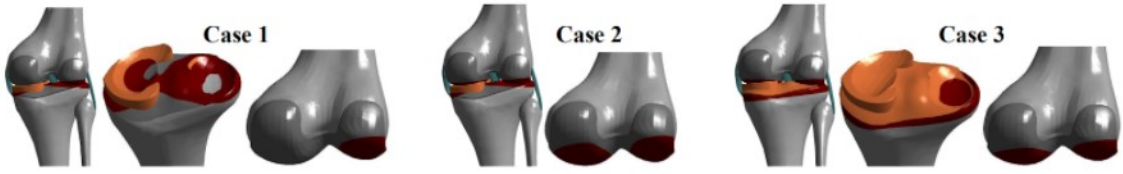

Figure 34. The three considered cases for the valgus inclination of 10° [46].

For geometric discretization Solid 186 tetrahedron elements defined by 20 nodes and Solid187 tetrahedron elements, defined by 10 nodes, have been used. The mesh of the geometric models for both the healthy and the OA knee have shown in **Fig.35**.

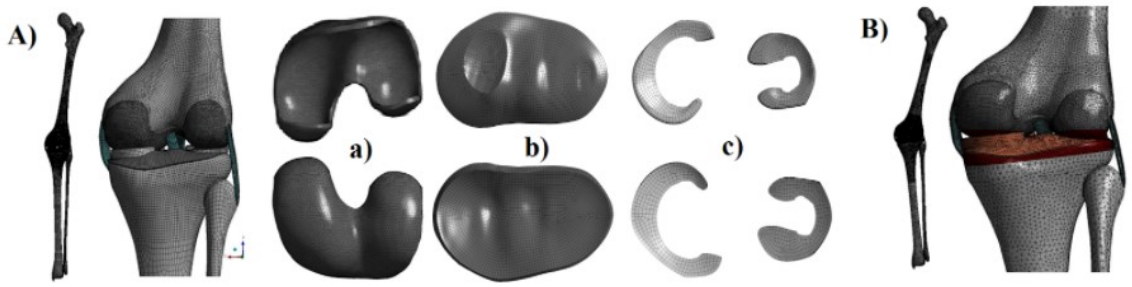

Figure 35. FE model for A) Healthy knee joint; (a) femoral cartilage; b) tibial cartilage; c) menisci; B) valgus knee joint [46].

For the FEA three different boundary conditions have been considered: 1) on the proximal head of the femur an 800N force and 1500N force in the Z-axis direction have been applied; 2) on the same location, a Remote Displacement is applied to allow offset Z and RotY around the femur; 3) on the tibia distal head Remote Displacement which allows RotY is applied as shown in **Fig. 36**.

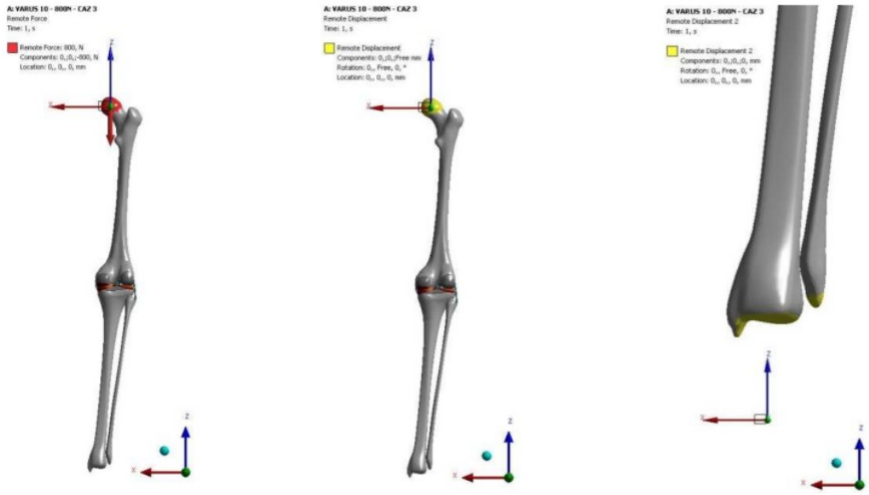

Figure 36. Boundary conditions applied for the numerical simulation [46].

Sun et al. (2016) [13] have applied the FEA to analyse the CF and their locations on the tibial plateau of an obese child with VD and a healthy child. The femur-tibia angle of

the left valgus knee from the obese child was 13°. From the CT image, the 3D FE model of the valgus knee was constructed, while the normal knee model was constructed using MR images. After the identification and segmentation of the bones and soft tissues in MIMICS v16.0, the 3D models were then assembled and meshed into 3D 4-node tetrahedral elements using ABAQUS v6.13-4. All materials were assumed isotropic, homogeneous, and linearly elastic to analyse contact stresses. The material properties used in this study have been listed in **Table 4.**

Table 4. Material properties of Sun et al. study [13].

Material	Young modulus (MPa)	Poisson's ratio
Femur	17.000	0.3
Tibia	12.200	0.3
Fibula	15.500	0.24
Patella	15.000	0.3
Cartilage	5	0.46
Meniscus	59	0.49
Ligament	6	0.4

Frictionless contacts with finite sliding were established between femoral cartilage with tibia cartilage and femoral cartilage with the meniscus. The other contacts were applied as tied contacts. Then the boundary conditions were set: the proximal end of the femur was fixed, and the tibia and fibula bear the load of Ry2 (**Fig. 37**).

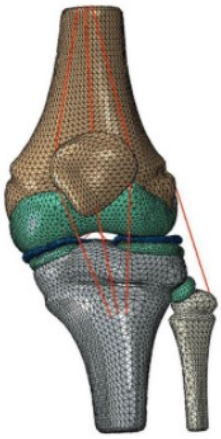

Figure 37. (a) Finite element model of knee valgus child's left knee [13].

Then, the nephrograms of Von-Mises stresses and contact stresses of the valgus knee were obtained as is shown in **Fig. 38**.

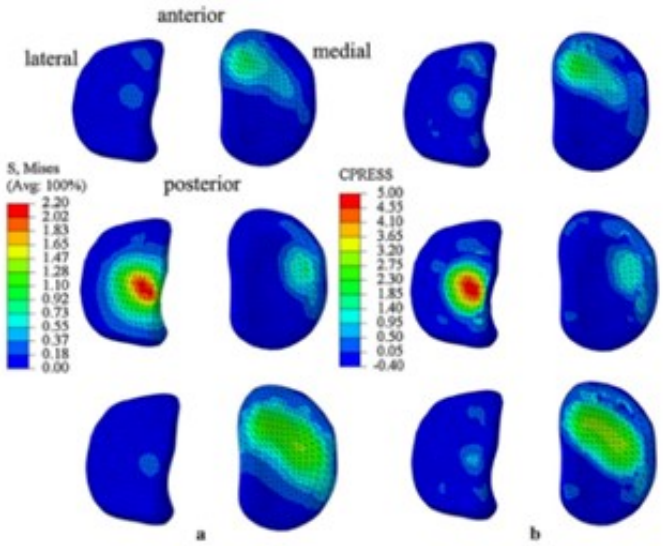

Figure 38. For the valgus knee model: a) nephograms of Von-Mises stresses; in b) nephograms of contact stresses [13].

3.3 FEA 3D knee model with ligament assumption

The complexity to elaborate the 3D knee model with several components integrated has led the researchers to find a way to make some simplifications reducing the computational time. To reach this goal, the ligaments components have started to be modelled in different configurations (1D, 2D, and 3D). Halonen et al. (2016) [47]have applied the assumption of ligaments as spring (Figure 46) in their study to simulate the effect of ACL rupture and reconstruction techniques on the knee joint motion as well as strains and stresses in the tibial cartilage during the stance phase of gait. Specifically, the ligaments have been assumed to be in tension at their normal length and thus a pre-strain of 5% has been applied to ACL and PCL and 4% to the LCL and MCL. These pre-strains have been implemented in Abaqus using the nonlinear spring response command. The values used during the simulation have been reported in **Table 5.**

Table 5. Material properties of the components modelled as spring in Halonen et al. work [47].

Material	Stiffness (N/mm)
ACL	201
PCL	258
MCL	114
LCL	134
QT	475
PT	545

The lateral patellofemoral ligament (LPFL) and medial patellofemoral ligament (MPFL) respectively were defined as linearly elastic elements with no compressive stiffness. Then the finite element model has been shown in **Fig. 39**.

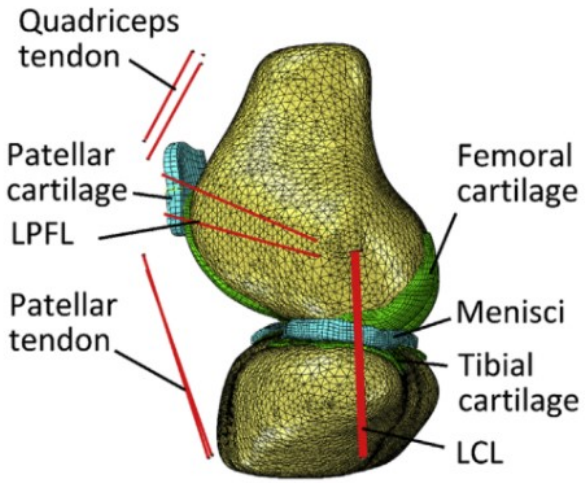

Figure 39. Sagittal view of the finite element model [47].

FEA has been also used to determine the magnitude and location of contact forces on the tibial plateau during gait patterns which have been recognized as a marker for risk of OA. Orozco et al. (2018) [48] have investigated the effect of five different constitutive representations of ligaments (spring, elastic, hyperelastic, porohyperelastic, and fibril-reinforced porohyperelastic (FRPHE)) on knee joints during the stance phase. Starting from a previously developed finite element model, they have segmented PT and QT, and ligaments (ACL, PCL, MCL, LCL, MPFL, and LPFL) as it is shown in **Fig. 40.**

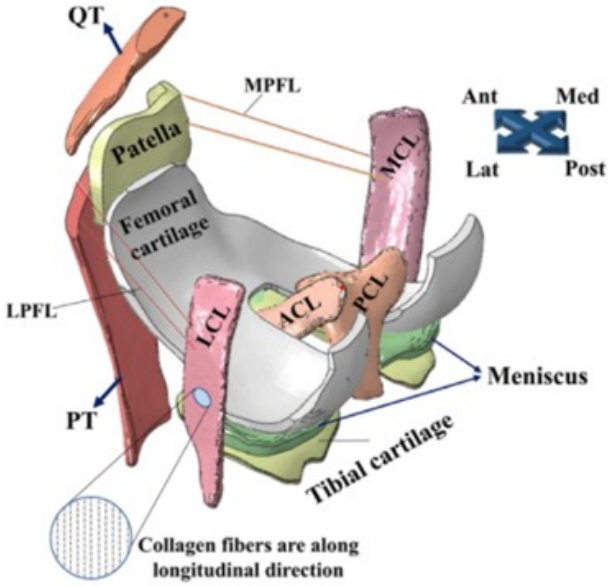

Figure 40. Posterior-lateral view of the three-dimensional finite element model of the knee [48].

Till today, biomechanical engineering works have explained several clinical disorders, but unfortunately, OA is one disease that continues to be not fully investigated. Indeed, although the finite element studies have improved the understanding of the knee joint structure, these computational models have not contributed to enhancing the treatment of knee conditions, e.g., in the case of knee OA, the biomechanics of which is still one of the unanswered research fields. In 2019, Abidin et al. [14] have published a work in which the FEA has been applied to analyse human knee joints. Starting from CT data of a healthy male, the bones have been reconstructed using Mimics (software version 10.01, Materialise, Leuven, Belgium). After, finite element models of bones and cartilages were then imported into 3-Matic for mesh editing. Two different degrees of knee flexion which are at 0° and 30° of flexion have been applied in this study. Then, the geometrical and mechanical properties have been assigned to the finite element model into MSC. Marc Mentat. The ligaments have been modelled as four ligaments at the knee joint. The stiffness coefficient (K) value of each ligament has been ranged from 20 to 75 N/mm. To make full knee extension, some compression loads from 100 to 1000 N have been applied axially on the femur. Meanwhile, 35 N of compression load has been assigned for the knee joint model with different knee flexion as reported in **Fig. 41**.

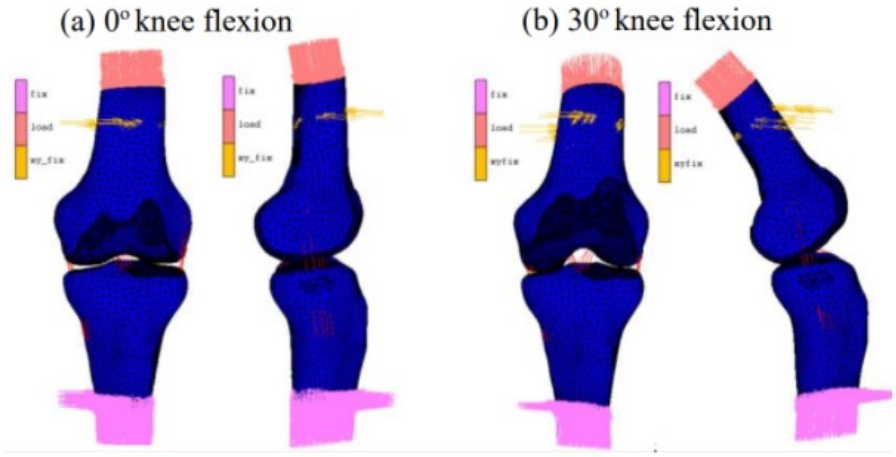

Figure 41. FEM of knee joint considering boundary conditions of 35 N compression load and fixed displacement at two different knee flexions; (a) flexion of 0°, (b) flexion of 30° [14].

From the FEA, the contour plot of peak Von Mises Stresses of articular cartilages of knee joint has been carried out in Figure 42 and they have been compared with previous literature work (**Fig. 42**).

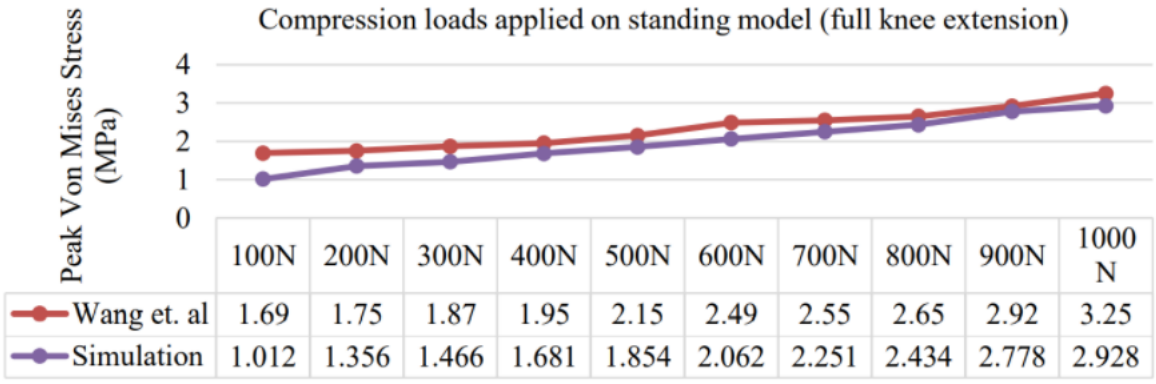

	100N	200N	300N	400N	500N	600N	700N	800N	900N	1000 N
Wang et. al	1.69	1.75	1.87	1.95	2.15	2.49	2.55	2.65	2.92	3.25
Simulation	1.012	1.356	1.466	1.681	1.854	2.062	2.251	2.434	2.778	2.928

Figure 42. Comparison of peak VMS between Wang et al. study and the Abidin et al. one [14].

As it has just been reported, many studies have focused on the application of FEA to investigate the Von Mises stress and strain parameters in the knee joint and in the knee TKA prosthesis; however, no works about how these parameters are distributed in the case of VD during an extension knee and then in the prosthetic knee implants.

3.4 FEA model to analyse the patellofemoral joint

The FEA has also found wide application in the study of patella instability. Watson et al. [49] have applied the FEA to examine patellofemoral biomechanics and patellofemoral contact pressures before and after MPF ligament reconstruction in the setting of patella Alta and Baja and concomitant also analysing the effects of the MPF ligament insertion site. A previously validated patellofemoral finite element model was modified to apply the specifications of the study. Bones have been modelled as rigid structures while the cartilage, patellar tendon (PT) and quadriceps tendon (QT), MPF ligament, and the medial patellotibial ligament (MPTL) have been modelled using 8-noded hexahedral elements. The cartilage was considered as a linear elastic material, the tendon and ligaments were modelled as hyperelastic. Four different patella heights have been accounted for by translating the "normal" model of the patella. The Caton-Deschamps Index ratio was 1.036 for "normal" patella, 1.2 for patella Alta, and 0.8 for patella Baja (**Fig. 43**).

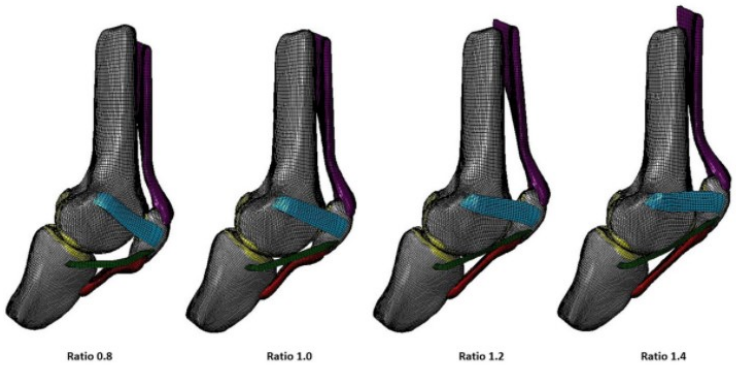

Figure 43. Patella baja (Caton-Deschamps 0.8), "normal" (Caton-Deschamps 1.0), and patella alta (Caton-Deschamps 1.2 and 1.4) finite element models [49].

In addition, each patella height model has been also modified to study multiple MPFL reconstruction insertion sites. For each patellar height and MPFL insertion site, the knee has been placed at 30° of flexion with the femur fixed in all directions. The tibia was free to translate and rotate around the anterior-posterior axis (z-axis) and the patella has been set free to rotate and displace in all directions. A load of 178 N has

been applied to the quadriceps and a lateral displacement of 10 mm for the patella was obtained. The analyses were then completed in Abaqus/Standard (Version 6.12-1; Dassault Systèmes Simulia, Providence, RI).

Woiczinski et al. [38]have used a fixed bearing CR TKA design to compare differences between the kinematics and load transfer in the same knee with axial internal/external rotation of the femoral component (CoRo) versus a separate trochlear groove rotation (TrRo). The FEA has been conducted in Ansys V14 software.

The starting point of the FEA was a geometric 3D model of the lower extremity of a healthy person. For all the simulation models, a fixed-bearing CR TKA prosthesis was virtually implanted under the control of an experienced orthopaedic surgeon. The ligaments were modelled as linear spring elements; the femur, tibia, patella, and femoral components were rigid bodies while the inlay and patella cartilage were deformable bodies. The material's properties have been listed in **Table 6.**

Table 6. Material properties of each componentable [38].

Material	Young's modus	Poisson's ratio	Density (g/cm^3
Femoral component	217.000	0.3	8.04
Inlay	312.5	0.46	0.93
Patella cartilage	5.0	0.46	1.00

The patellofemoral and tibiofemoral contacts were simulated with friction coefficients of 0.02 and 0.05. A coordinate system was established in full extension at the distal tibia with Z-axis pointing to the femoral head, X-axis aligned parallel to the mediolateral transepicondylar axis of the femur. The knee was free to move in all DOFs. A knee squat modelled flexion of up to 105° within 60 load steps. For every single load step, a ground reaction force was between 50 and 55 N. Then, the modifications of the axial femoral component rotation (CoRo) and the designed trochlear rotation (TrRo) have been implemented in Catia V5R19 software and have been tested in the FEA knee model.

Different axial internal/external rotation angles of 3° internal, 3° external, and 6° external rotation have been simulated as shown in (**Fig. 44**).

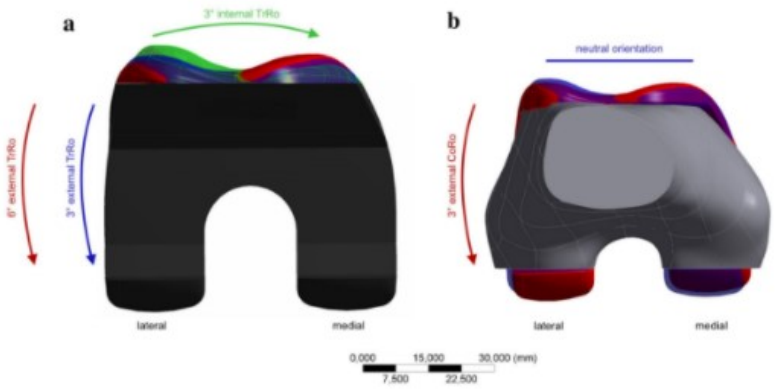

Figure 44. (A)Trochlear groove rotation within the femoral component design; (B)Axial femoral component [38].

The kinematics of the patella has been analysed (**Fig. 45**). Then, it has been demonstrated that an external trochlear groove rotation in TKA design can reduce the patellofemoral stress avoiding anterior knee pain.

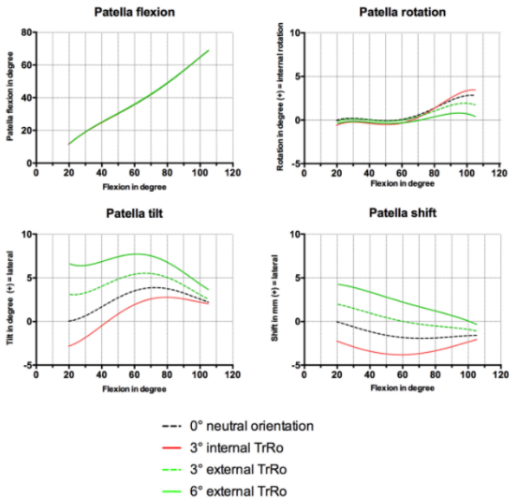

Figure 45. Patellar kinematic changes caused by the trochlear rotation [38].

Even though the previous works have largely applied the FEA in the field of prosthesis, some aspects remain unknown. Thus, the present work aims to apply the FEA in the case of valgus knee misalignment to assess the pitfalls of the TKA.

4 Materials and methods

In this section, it will be presented the workflow of the present study divided in three parts. The first part has regarded the acquisition of knee bone geometries and prosthetic components. In the second part have been reported all the steps to reconstruct the valgus knee model and then to simulate the TKA procedure. In the last part, the planning of the FEA has been introduced and then the simulation has been performed. All the steps have been simplified in **Fig. 46**.

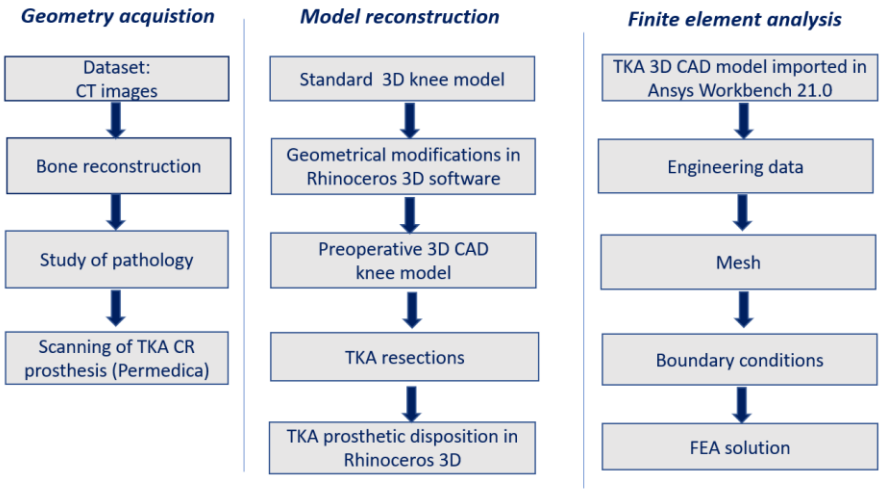

Figure 46. Workflow of the present study.

4.1 Geometry acquisition

In this work, a list of the patients who have undergone TKA procedures in Ospedale Riuniti Ancona, from 2017 to 2021 was consulted. Among the patients, the CT scans of the knee with VD were considered to make clinical observations about the pathology. Specifically, two medical CT images of a female subject (age=88 years) and a male subject (age=80 years) affected by primary OA have been included. In both cases, on the left knee, it was already implanted a Hinged prosthesis on the female subject and a CR prosthesis on the male one respectively, as is shown in **Fig. 47**.

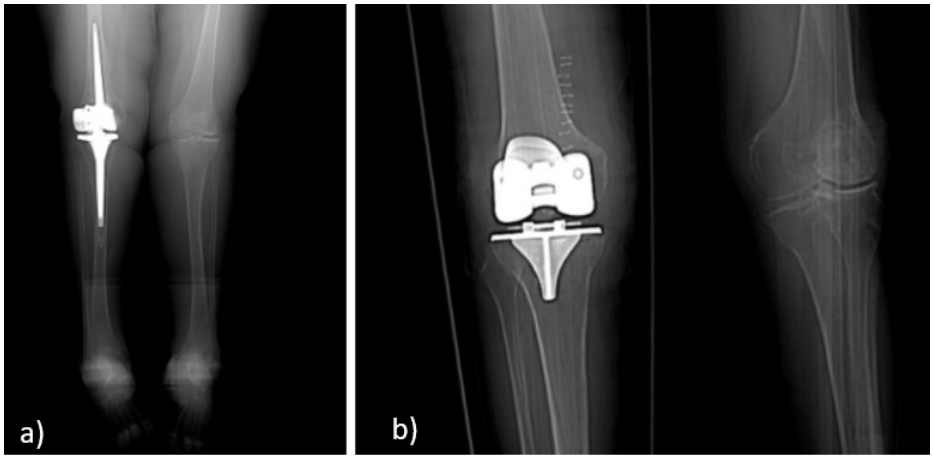

Figure 47. a) Hinged prosthesis implanted on the female patient; b) CR prosthesis implanted on the male patient.

The CT data were imported into an image processing software for 3D design and modelling. The thresholding procedure was used to segment the DICOM files defining three masks: femur, tibia, and patella (**Fig. 48**). In this case, a predefined threshold set (bone) with a range of intensity between 226 HU (minimum value) and 3071 HU (maximum value) was selected as it is illustrated in Figure 48. Then, a 3D model of the bones structure was constructed as shown in **Fig. 49**.

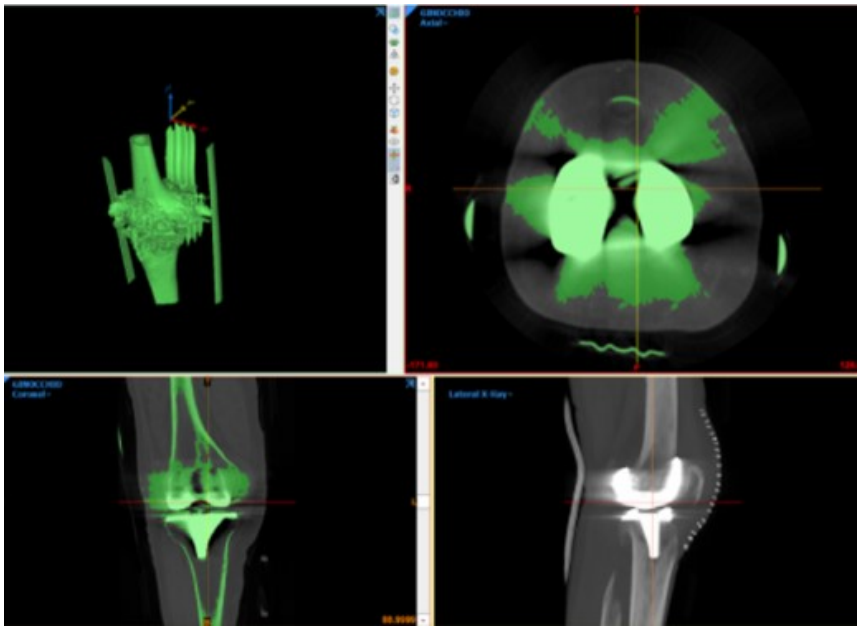

Figure 48. Thresholding procedure in Mimics Medical 21.0.

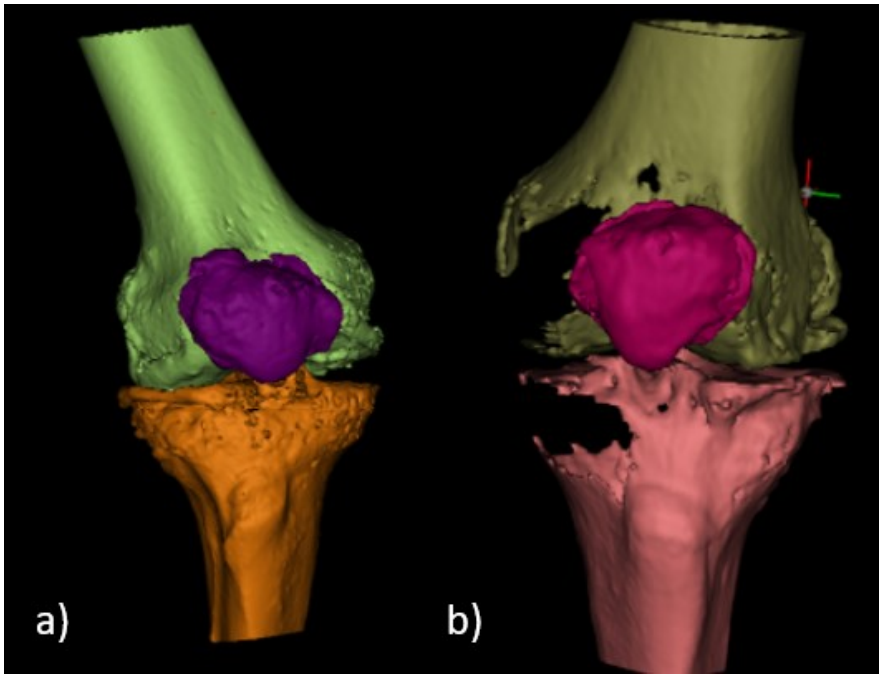

Figure 49. Bones reconstruction after mask creation: a)male subject; b) female subject.

A total compartmental prosthesis called GKS Prime Flex CR prosthesis (Permedica) has been chosen. This prosthesis implant was composed of three components: the femoral component made of chromium-cobalt alloy, the tibial component made of titanium alloy, and the insert made of UHMWPE. The geometries of each prosthetic component have been scanned in the laboratory using a Go!Scan, a very powerful tool characterized by an high accuracy and level of details. Once the scanning was completed, post-processing was made to improve the quality of the imported components **(Fig. 50- Fig.51**).

Figure 50. Pre-scanning of the TKA components: a) femoral component; b)insert; c) tibial component.

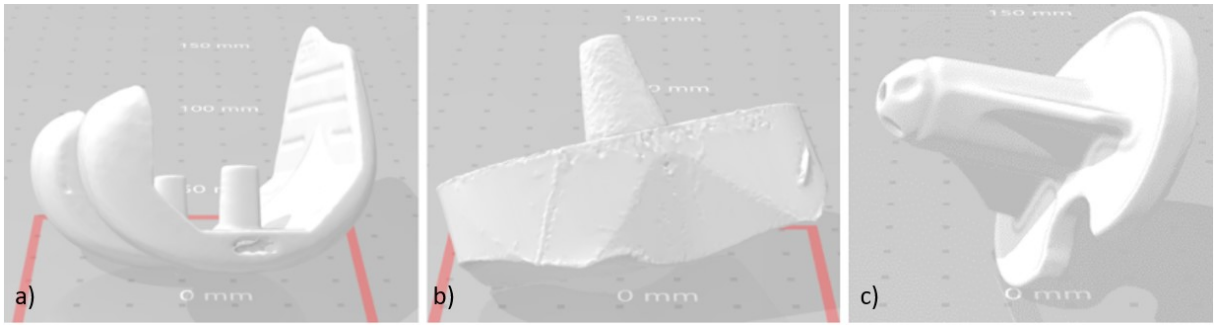

Figure 51. Post-scanning of the TKA components: a) femoral component; b) insert; c)tibial plate.

4.2 Model reconstruction

The second phase of this work was the model reconstruction of the knee joint. After applying the thresholding procedure, it was not possible to achieve a completely reconstruction of the knee bones and soft tissue. Thus, these models have been used to study the VD and the anatomy of the knee joint, but the starting point to construct the final knee model has been a predefined standardized knee geometry designed on CINEMA 4D 18 software. This model is characterized by 10,000 polygons, 1,000,000 vertices and it is in the flexion position (**Fig. 52**).

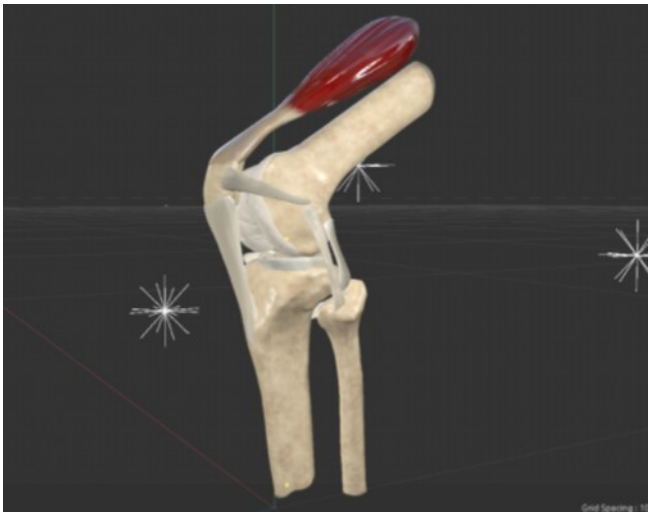

Figure 52. Standardized knee geometry in Cinema 4D 18 software.

Specifically, the model is composed of the following structures: femur, tibia, patella, fibula, femoral cartilage, medial and lateral menisci, QT, PT, MCL, LCL, PFL, LPFL and MPFL. This standard model was imported in Rhinoceros 3D software to modify the geometries of some components in order to obtain a valgus knee in the extended position. Considering closed chain kinematics, the tibia has been considered fixed while starting from the initial position (flexed knee), the femur, the patella, femoral cartilage, LPFL and MPFL have been rotated of 60° to obtain an extended knee position. Firstly, a rotation of 60° was made for the femur, patella, femoral cartilage, LPFL, and MPFL to pass from flexed knee to the extended one. Consequently, the MCL, PFL, tendons, and menisci were remodeled under the examination of an experienced orthopedic surgeon. The tibia was scaled so that a gap between menisci and femoral cartilage was removed. Since the simulations are performed with the leg in full extension, the fibula and LCL have been not taken into consideration for this analysis (**Fig. 53**). Additionally, after the rotation has been performed, the calculation of the femoral-tibial angle has revealed a valgus angle of 20.1°.

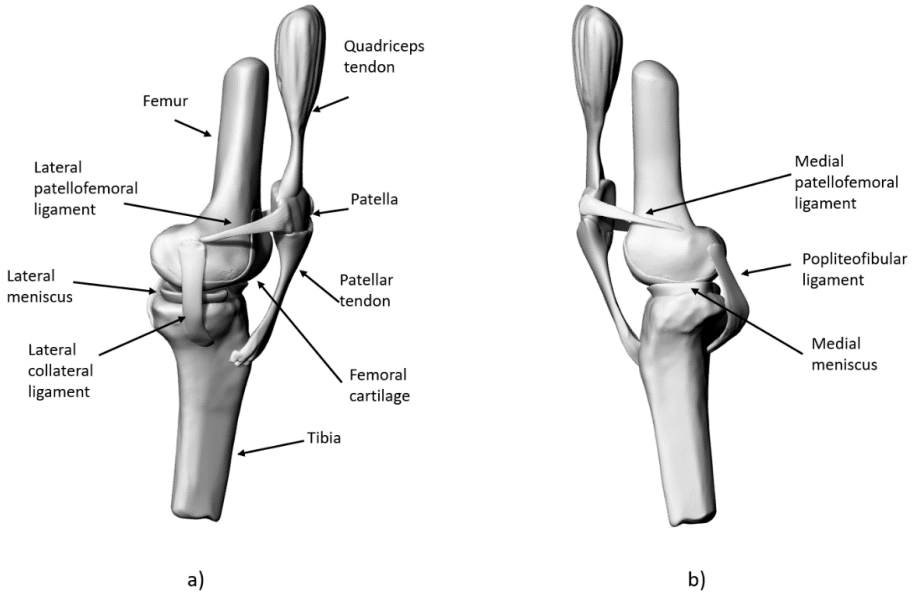

Figure 53. Extended knee with VD obtained in Rhinoceros 3D software: a)lateral side; b)medial side.

Then, the ACL and PCL have been created starting from the PFL shape. The ACL was placed on the medial part of the external horn of the meniscus until the medial condyle while, PCL was placed on the posterior part of the tibia until the lateral face of the lateral condyle (**Fig. 54**).

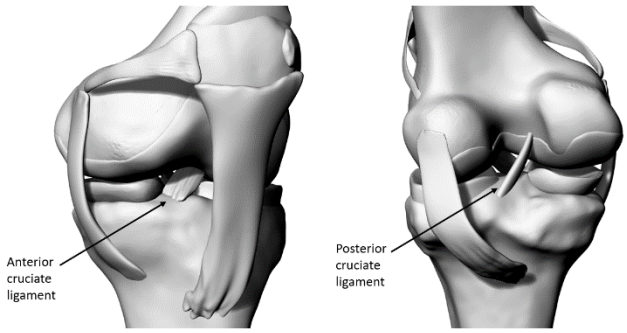

Figure 54. ACL and PCL constructed in Rhinoceros 3D software

A fitting tool was used to convert the mesh to a NURBS surface using a reverse engineering processing software. Thus, the final surface was a NURBS surface solid model, which is exported in IGES format. Finally, a 3D geometric entity model of the valgus knee joint in extension position was constructed and it has composed of femur, tibia, patella, surface cartilage, medial meniscus, lateral meniscus, ACL, PCL, MCL, LCL, MPFL, LPFL, and PFL created in Rhinoceros 3D software. The preoperative standard model has been again imported in Rhinoceros 3D software to make some changes before the implantation of TKA components. Firstly, the patella has been brought close to the femur. Then, the femoral cartilage and menisci have been removed to simulate the TKA procedure. According to the planning of the TKA procedure, the resections of the femur and tibia have been made using NX SIEMENS software. Specifically, the tibial tray has been resected by fixing a plane tangent to the superior surface of the tibial insert and offsetting it along the Z-axis of -3 mm (dimension of tibial insert thickness). This plane has been used to cut the tibia and to obtain the resection (**Fig. 55**). The same procedure was used for the femoral component.

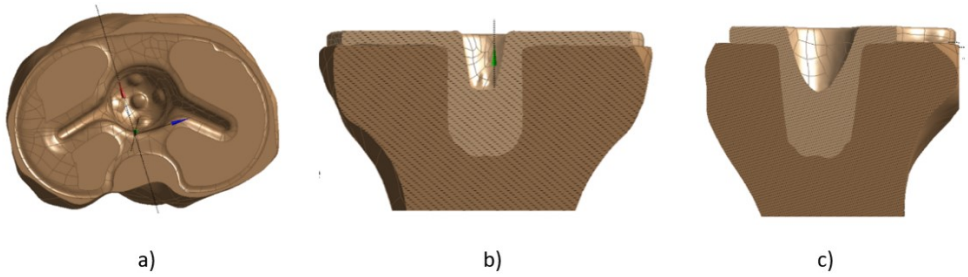

Figure 55. Tibial resections: a) top view; b) frontal view; c) sagittal view.

Once the resections have been created, the prosthesis implants have been implanted: the femoral component has been placed in contact with the femur to substitute the damaged femoral cartilage; the tibial tray has been inserted in the tibial resections to substitute the menisci and the insert has been arranged over the tibial tray. Finally, the postoperative geometric knee model has been created and exported in the .stl file.

4.3 Finite element analysis

The next step of the present study was a static structural FEA developed in Ansys Workbench 2021 R2. The 3D knee model was imported in Ansys Design Modeler to generate the fourteen solid bodies measured in mm. The materials have been defined as isotropic, homogeneous, and linearly elastic according to [13]. The elastic Young modulus and Poisson's ratio for each knee component have been listed in **Table 8**.

Table 8. Material properties used in the present study according to [13] and [50].

Material	Young's modulus (MPa)	Poisson's ratio
Femur	17.000	0.3
Tibia	12.200	0.3
Patella	15.000	0.3
Femoral component	210.000	0.3
Insert	685	0.4
Tibial tray	117.000	0.3

Three bonded contacts have been defined between femoral component and femur; tibial plate and tibia; tibial plate and insert allowing no sliding and no separations between the target and the contact. Non-linearity was done by the existence of nonlinear contacts. All the contacts have been shown in **Fig. 56**.

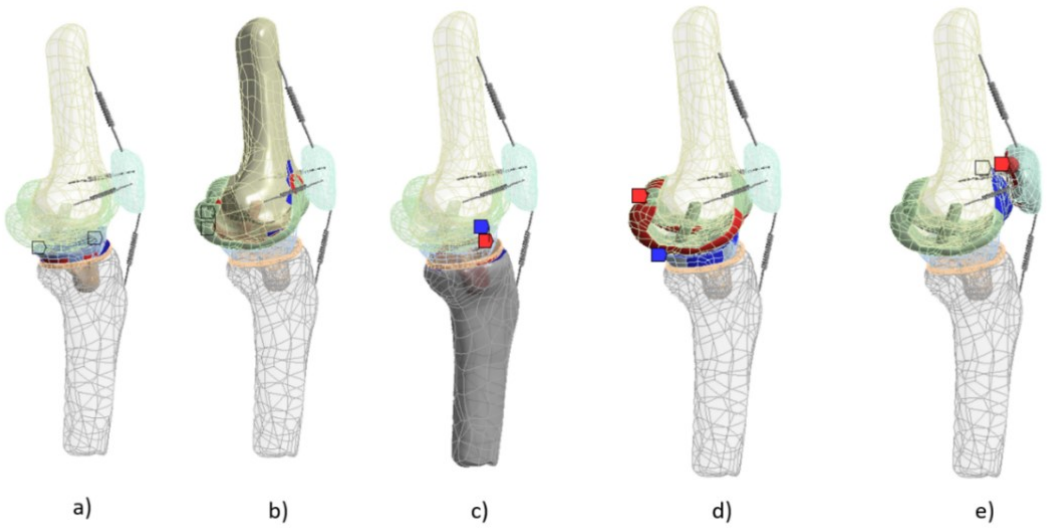

Figure 56.Bonded contacts defined during the simulation: a) between tibial plate and insert; b) between femur and femoral component; c) between tibia and tibial plate; frictional contacts: d) between femoral component and insert; frictionless contact: e) between patella and femoral component.

Specifically, frictional surface-to-surface contact has been applied between the femoral component and insert with a frictional coefficient of 0.2 and a Normal Lagrange calculation algorithm was chosen. Frictionless surface-to-surface contact has been set between the femoral component and patella using Augmented Lagrange. A setting called "Normal Stiffness Factor" (NSF) analysis, a normal multiplication factor used to control the amount of penetration between contact and target surfaces, has been introduced. Usually, higher normal stiffness values decrease the amount of penetration but can lead to convergence difficulties. On the contrary, lower normal stiffness values can provoke a certain amount of penetration and produce an inaccurate solution. Thus, after some attempts, the normal stiffness factor has been chosen equals to 0.0001. For a more efficient mathematical representation of the contact

areas, the option “Pinball Region” with a different radius according to the contact status tool was used to close the geometrical gaps. Two local references system have been inserted, one for the femur component and the second one for the patella following the conventions presented in [51]. Considering the large number of nodes and elements but, also the presence of nonlinear contacts, for solving the analysis it has been implemented a “smaller steps” system using the Auto Time Stepping. Due to the complexity of knee ligaments consisting of elastic bands of soft tissues, a wide range of element types and material models have been found in literature to easily represent their biomechanics [52]. Among them, the line elements such as springs have been considered to facilitate the representation of the knee ligaments. Specifically, they have been assumed as longitudinal only tension springs without pre-strains with the corresponding stiffness: 475 N/mm for QT; 545 N/mm for PT [48]. while 16 N/mm for MPFL; 12 N/mm for LPFL according [53]. Specifically, the spring of PT was oriented from attachment points on the distal patella to the tibial tuberosity; the QT spring was placed from the superior extremity of the femur to the top surface of the patella; while the MPFL and LPFL springs were attached from the medial/lateral facet of patella to the medial/lateral femoral condyles, respectively as shown in **Fig. 57**.

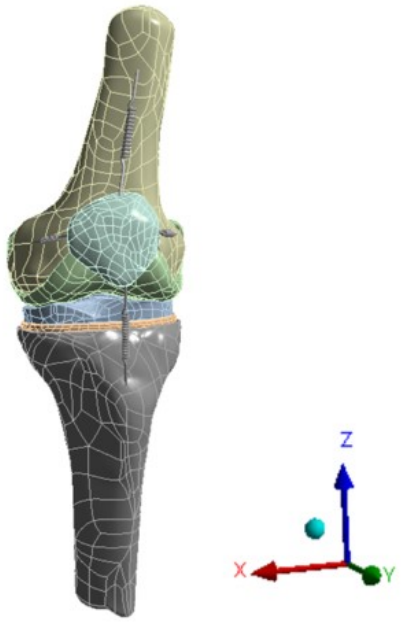

Figure 57. Spring elements used to model knee ligaments.

In order to replicate the flexion movement, three different boundary conditions have been selected. Firstly, the tibia has been fixed at its distal end to avoid any movements; secondly, a remote displacement has been applied to the femur head to constrain the rotation along the flexion-extension axis (x-axis) while the other rotations and traslations have been setted as free. By choosing two nodes along the medial and lateral femoral condyles, the nodal displacement has been inserted to offset the displacement along x, y and z directions. In particular, for this examination only the rotation knee mechanism has been considered while any translation has been neglected. The three boundary conditions have been shown in **Fig. 58**.

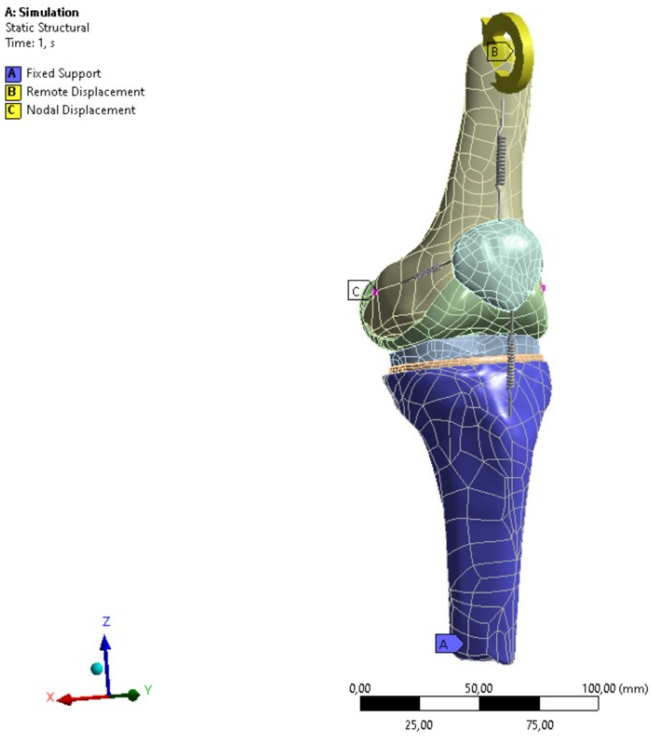

Figure 58. Boundary conditions.

Once contacts and boundary conditions have been defined, the mesh analysis was conducted by choosing the most suitable mesh element for the current study. The use of smaller elements allows achieving a more accurate discretization, fitting better the original shape, and improving the accuracy of the outputs. Unfortunately, the rise of the number of nodes and consequently the number of equations, also increases the computational time.

Therefore, a trade-off between computational time and accuracy has been considered. In this case, the geometries have been all meshed with linear tetrahedral elements as is shown in **Fig. 59**.

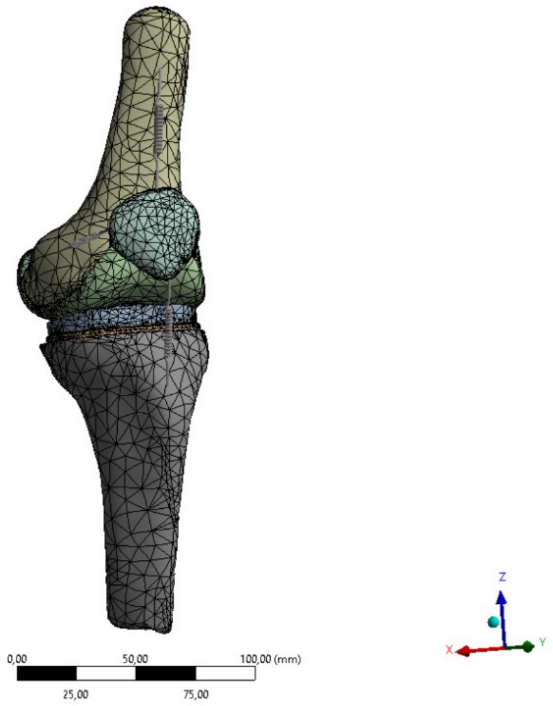

Figure 59. Mesh.

The total number of nodes and elements for each knee components have been listed in **Table 7.**

Table 7. Nodes and elements of the 3D TKA model.

Structure	Nodes	Elements
Femur	16474	9401
Tibia	14873	8674
Patella	3478	1896
Femoral component	9183	4789
Insert	7118	6770
Tibial tray	12476	6770

5 Results

This chapter reports all the results achieved during the static structural analysis. It has been analysed the patella kinematics, the contact pressure between femoral component and patella, and finally the von Mises stresses of the insert.

5.1 Patella kinematics

The first qualitative assessment of patella kinematics has been obtained by considering its volume during three different time steps of the simulation as is shown in **Fig.60-Fig.61**.

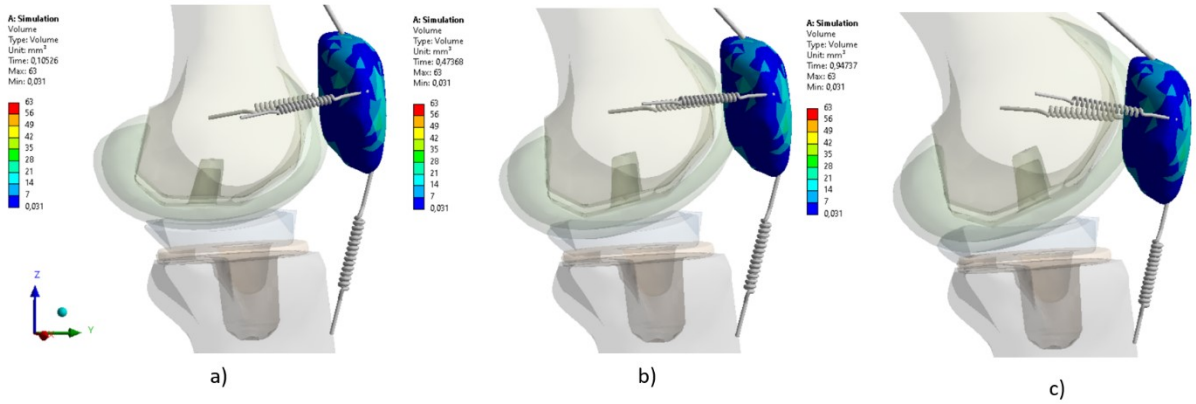

Figure 60. Frontal view of patella at three time steps of simulation at 38° of femur knee flexion.

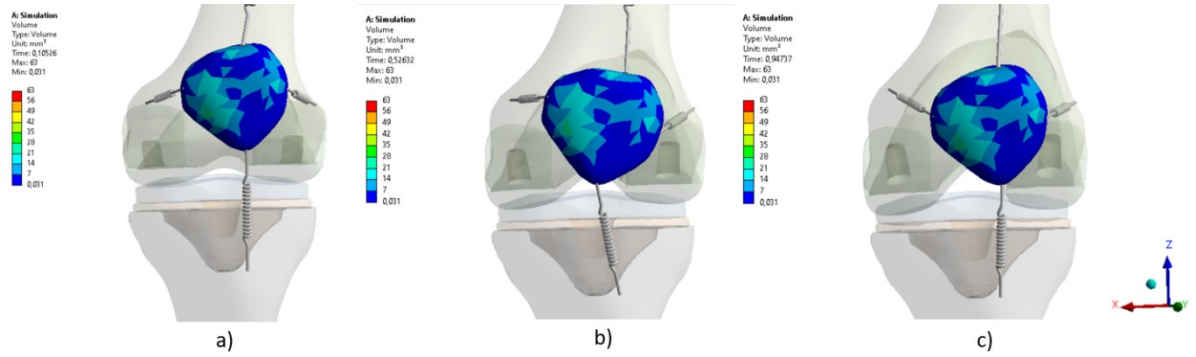

Figure 61. Sagittal view of patella at three time steps of simulation at 38° of femur knee flexion.

Now, in the following figures (**Fig. 62- Fig. 63-Fig.64**) it is possible to appreciate the displacements of the patella during the flexion femur movement along the three axes (anterior-posterior, medio-lateral and vertical axes).

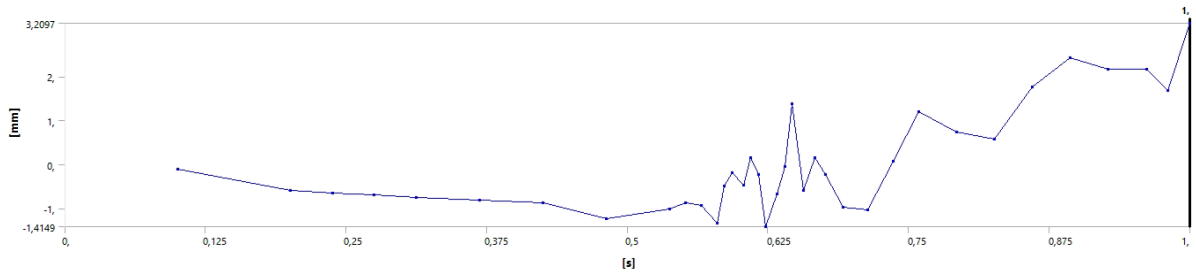

Figure 62. Patella translations along the anterior-posterior axis.

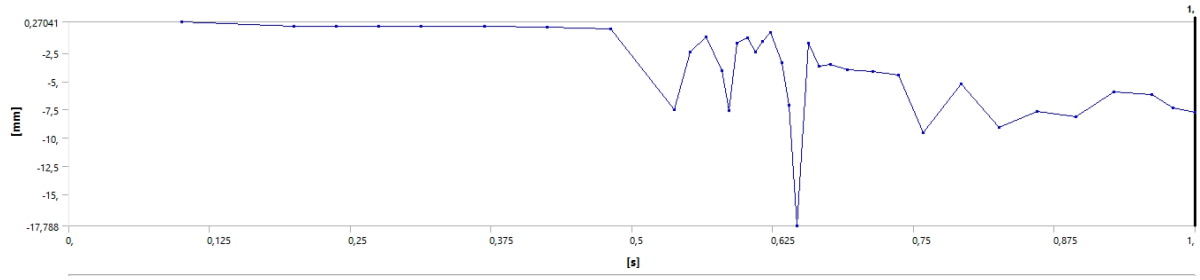

Figure 63. Patella translation along the medio-lateral axis.

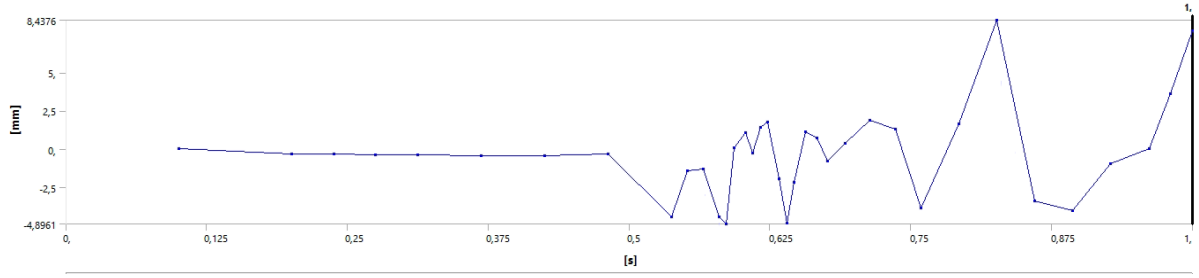

Figure 64. Patella translation along the vertical axis.

At the same way, the patella rotation movements have been assessed and reported in the following figures: **Fig. 65-Fig.66-Fig.67**.

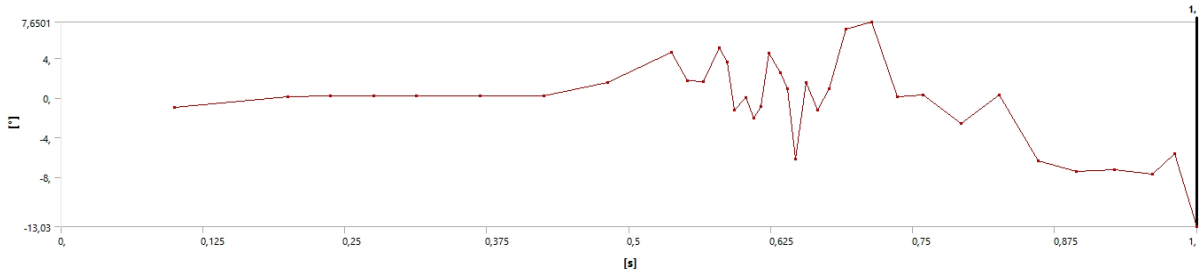

Figure 65. Patella rotation along the anterior-posterior axis.

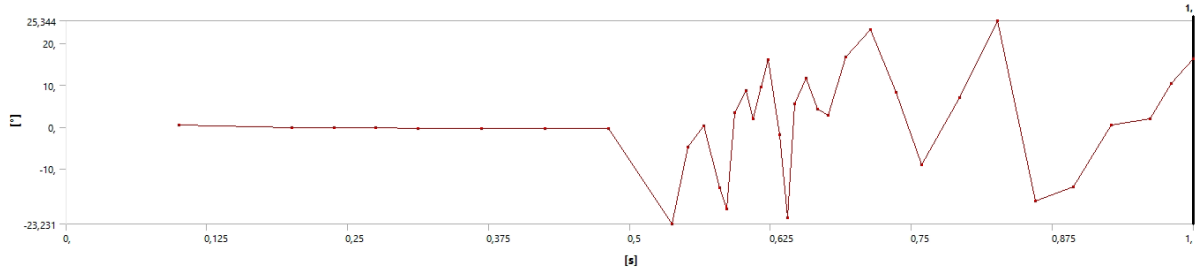

Figure 66. Patella rotations along the medio-lateral axis.

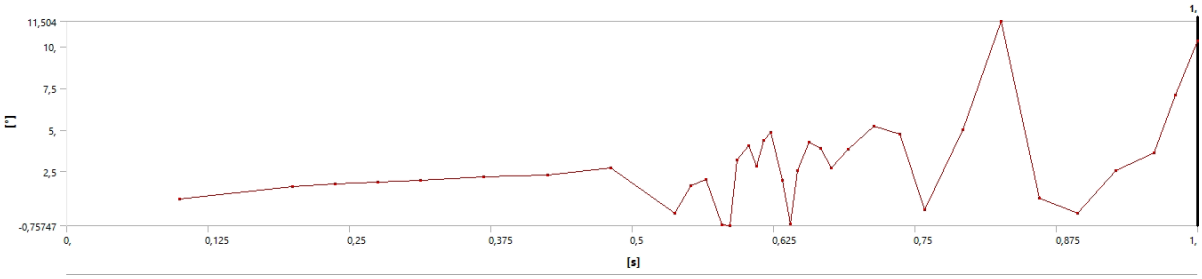

Figure 67. Patella rotations along the vertical axis.

5.2 Patellofemoral contact pressure

The contact pressure between the patella and femoral component have been computed at three flexion angles. At 15° of knee flexion, the contact pressure is 0 MPa. At 38° (maximum flexion angle reached by the femur) of knee flexion, the maximum contact pressures was 1.24 MPa. The representative patellofemoral joint contact pressure profiles are shown in **Fig. 68-Fig.69**.

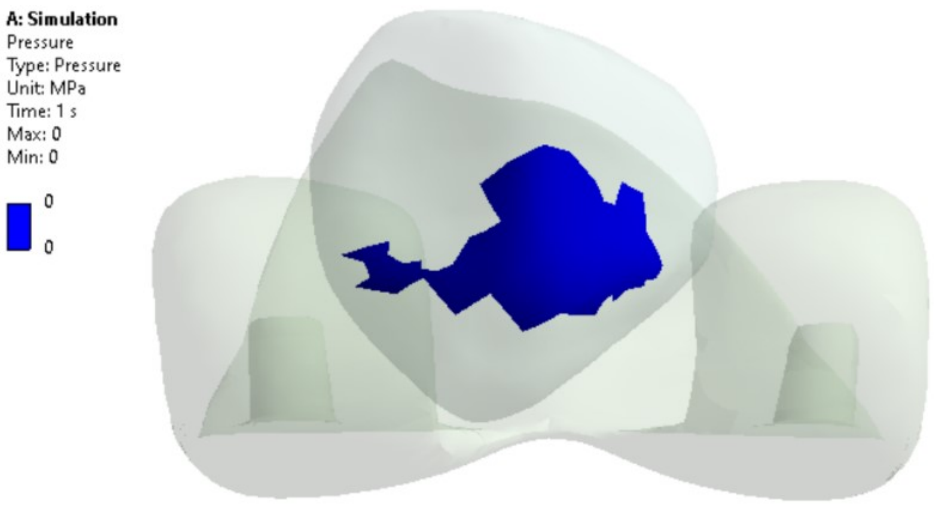

Figure 68. Patellofemoral joint contact pressure at 15° of knee flexion.

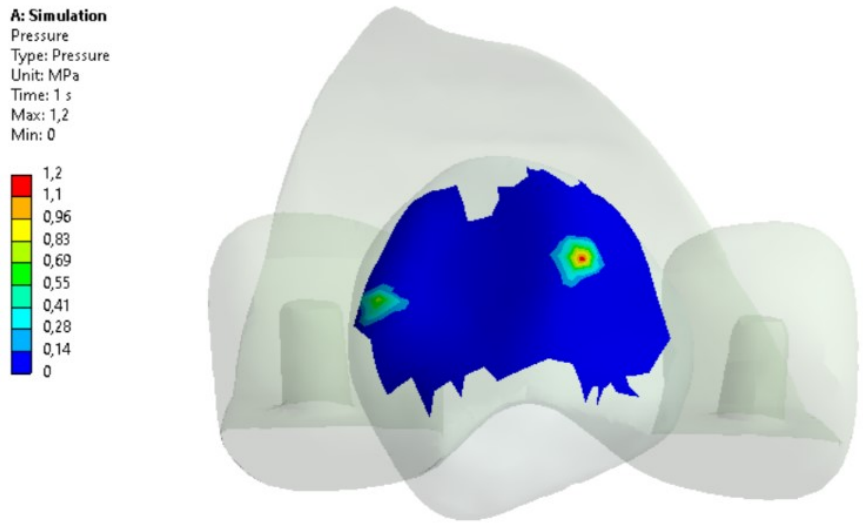

Figure 69. Patellofemoral joint contact pressure at 38° of flexion.

Additionally, from the number of contacting plot it has been assessed the time instant of simulation in which the first contact between the patella and the femoral component has occurred as illustrated in **Fig. 70**.

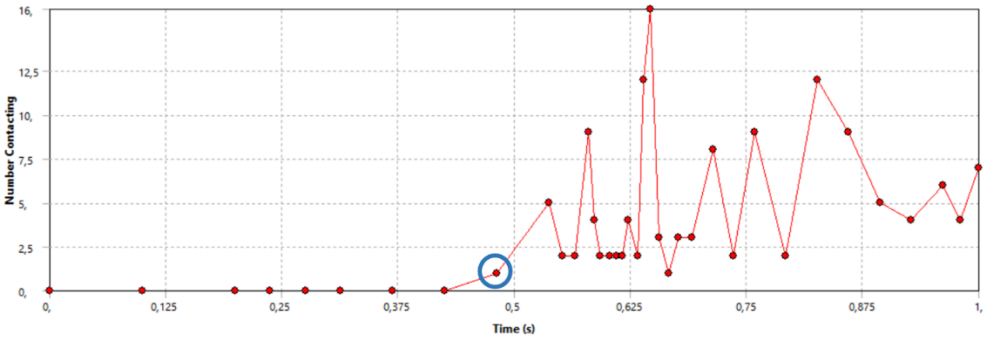

Figure 70. Number contacting plot. The blue circle indicates the exact time step instant of simulation at which the first contact between patella and femoral component has occured.

Then, using a flexion rotation probe it has measured the femur rotation at this time and it was 24.86°.

5.3 Von Mises stresses of insert

Similarly, to the contact pressure, the von Mises stresses have been computed for the same flexion angles. The maximum value of the von mises stress were 0.84 MPa, and 1100 MPa at 15° and 38° of knee flexion, respectively. The nephograms of von-Mises stresses are shown in the **Fig. 71-Fig.72**.

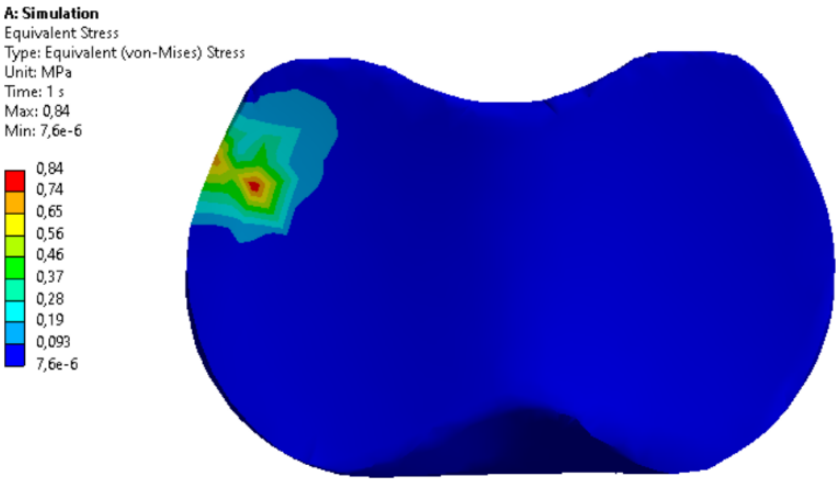

Figure 71. Nephograms of von-Mises stress at 15° of flexion.

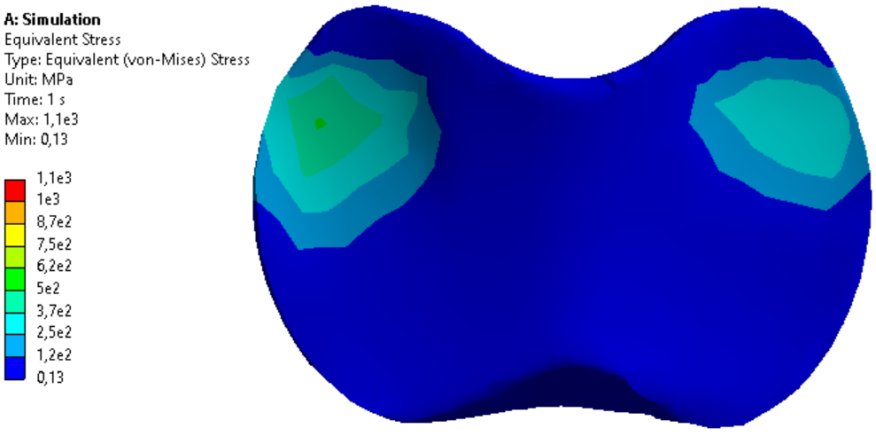

Figure 72. Nephograms of von-Mises stress at 38° of flexion.

6 Discussion

Total knee arthroplasty (TKA) is one of the most consistently successful surgeries performed in orthopedics. Despite this, patient-reported outcomes have shown dissatisfaction after the surgical procedure dramatically affecting their quality of life [54]. Among the patient's complaints, the anterior knee pain provoked by abnormal patellar tracking is the most frequent cause of revision rate. The complications of TKA have long fascinated the community proposing several works with FEA application. Although, FEA has been frequently applied to assess the field of prosthetic implants, until now there are not found studies focused on the dynamics of the postoperative knee joint in presence of valgus misalignment. Furthermore, it has been reported how the complexity of patellar geometry and its movements, makes it difficult to measure in vivo patellar tracking [54]. Thus, the present work aimed to develop a virtual knee model to investigate the patellar tracking in presence of VD after the TKA procedure. The results obtained from the FEA are encouraged. Firstly, the patella kinematics has been assessed by considering the volume occupied by the patella during the flexion movement. From Fig. 60-Fig. 61 it is possible to appreciate that at 0% of simulation, the patella was not in contact with the femoral trochlea while at 50% of simulation a first rubbing between them has occurred. At the end of simulation when the femur was flexed almost 38°, a bigger surfaces area of the patella was in contact with femoral trochlea. These findings have been consistent with the Fig. 62-Fig.63-Fig.64 in which have been shown the patella translations along the three axes. Specifically, it can be noted as before 0.5% of simulation, the trend in all the three axes has assumed a small variation, while when the first contact between patella and femoral component has been reached, the trend became sharper. In addition, as the flexion femur angle increased, the translation of the patella also has undergone more prominent changes. Along the anterior-posterior axis, the patella has translated from -1.4149 mm to 3.2097 mm; along the medio-lateral axis from -17.788 mm to 0.2741 mm; along vertical axis from -4.8961 mm to 8.4376 mm.

From **Fig.65-Fig.66-Fig.67** it is possible to note the patella rotations. As previously described for the patella translations, also in this case firstly the trend was smooth and then after the first contact between patella and femoral component, the patella has assumed a more irregular trend with higher peaks. More in detail, it has reached a range between -13.03° and 7.65° around the anterior-posterior axis; a range between -23.23° to 25.34° around the medio-lateral axis and -0.75° to 11.50° around the vertical axis. Thus, from these plots it has been demonstrated that the patella movement changes with the change of flexion angle. In the second section, it has been inserted the results regarding the contact pressure between the femoral component and patella. It has been pointed out from **Fig.68-Fig.69**, that the increase of contact pressure depends on the flexion angle. Indeed, the contact pressure measured at 38° (1.2 MPa) of flexion was higher than the ones measured at 15° (0 MPa). Moreover, it has been confirmed that at the maximum flexion angle reached by this model (38°), the patella was in contact with the femoral component since the contact pressure was high. Probably, the high values of contact pressure may be due to the high stiffness value of the ligaments. Starting from these observations, it has also been investigated the femur flexion angle at which the first contact has been presented. From the flexion rotation probe used in Ansys, it has been obtained an angle of 23°. This is faithful to the literature according to which the patella touches the femoral component at almost 20° of flexion [24]. Farrokhi et al. have demonstrated a similar result considering the contact between femoral cartilage and patellar one in the case of patients with patellofemoral pain[55]. The analysis of von Mises stresses on the insert has revealed an abnormal distribution between the lateral and medial plateau at all flexion angles. Sun et al. [13] have obtained similar results comparing the von Mises stresses in the healthy knee and valgus one. They have highlighted greater lateral stress in the valgus knee with respect to the healthy one. Even if, some of the obtained findings cannot be validated with other works, they could be used to compare the future simulations. From the reported results it can be inferred that the finite element model employed in this work can study the dynamics of the postoperative valgus knee. The patterns of the patella trajectory may help to understand if the use of CR prosthesis under this

clinical scenario, could offer stability and must be preferred with respect to other prostheses. Specifically, from the patella's displacements, it can be noted an irregular trend after the first contact between the femoral component and patella could induce instability. By combining this finding with the information regarding the flexion femur angle at the first contact, it could prospect if some CR femoral component modifications could ensure a smoother patella's tracking. Furthermore, the higher contact pressure which gradually increases with the flexion angles can be conceived as a major risk for the patients in case of more accentuated movements. The nephograms of von Mises stresses indicate higher stress distributed along the lateral side suggesting that the valgus knee could be the reason for abnormal knee load distribution. In summary, the present work has reached the goal: the FEA has been applied in case of VD, the patella kinematics has been studied and the obtained results could be compared with other examinations. In conclusion, the present work could be the starting point of further investigation aimed to improve the TKA outcomes reducing the risk of anterior knee pain for the patient.

7 Conclusion

This thesis presents a finite element model to give researchers and orthopedics a better understanding of the dynamics of the valgus knee after the TKA procedure. Indeed, the preoperative 3D CAD valgus knee model offers the possibility to practically understand the bones and ligaments remodelling in presence of OA phenomenon. The postoperative model is useful to explain how the TKA procedure is performed during surgery. Differently from the previously mentioned works, the FEA has been applied to study the patellofemoral joint in correlation with VD and which could be the possible complications of CR-TKA design. The proposed FEA model presents some limitations. Firstly, the design choice of spring elements to model tendons and ligaments offers from the one hand, the possibility to speed up the computational time of the convergence analysis, but on the other hand makes the biomechanical function of ligaments less realistic. Secondly, the femur has not achieved all the flexion movement during the simulation. These drawbacks could be easily resolved by considering 3D ligaments and other materials i.e., hyperelastic materials. In conclusion, this FEA model is revealed as a suitable tool for the purpose, obtaining heartening results. This may be a step toward new research aimed at the development of TKA designs able to reduce the patient's dissatisfaction.

8 References

[1] S. Affatato, *The history of total knee arthroplasty (TKA)*. Woodhead Publishing Limited, 2015. doi: 10.1533/9781782420385.1.3.

[2] A. Causero, P. di Benedetto, A. Beltrame, R. Gisonni, V. Cainero, and M. Pagano, "Design evolution in total knee replacement: which is the future?," *Acta biomedica : Atenei Parmensis*, vol. 85, no. September, pp. 5–19, 2014.

[3] F. Tian, X. H. Zang, and Y. S. Sun, "Impact of knee varus and valgus deformity on alignment in lower extremities after total knee arthroplasty (TKA)," *European Review for Medical and Pharmacological Sciences*, vol. 22, pp. 83–89, 2021, doi: 10.26355/eurrev_201807_15368.

[4] A. Boulos and N. Lemme, "Total knee arthroplasty," *Essential Orthopedic Review: Questions and Answers for Senior Medical Students*, pp. 165–168, 2018, doi: 10.1007/978-3-319-78387-1_74.

[5] G. Niccoli, D. Mercurio, and F. Cortese, "Bone scan in painful knee arthroplasty: obsolete or actual examination?," *Acta Bio Medica Atenei Parmensis*, vol. 88, no. 2-S, pp. 68–77, 2017, doi: 10.23750/abm.v88i2.

[6] C. Improvements, "Total Knee Arthroplasty: Past Successes and AND ABSTRACT," vol. 87, no. 1, pp. 161–162, 2008.

[7] J. N. Argenson *et al.*, "Survival analysis of total knee arthroplasty at a minimum 10 years' follow-up: A multicenter French nationwide study including 846 cases," *Orthopaedics and Traumatology: Surgery and Research*, vol. 99, no. 4, pp. 385–390, 2013, doi: 10.1016/j.otsr.2013.03.014.

[8] K. Toguchi *et al.*, "Predicting clinical outcomes after total knee arthroplasty from preoperative radiographic factors of the knee osteoarthritis," *BMC Musculoskeletal Disorders*, vol. 21, no. 1, pp. 1–8, 2020, doi: 10.1186/s12891-019-3029-7.

[9] J. Girard *et al.*, "Total knee arthroplasty in valgus knees: Predictive preoperative parameters influencing a constrained design selection," *Orthopaedics and*

Traumatology: Surgery and Research, vol. 95, no. 4, pp. 260–266, 2009, doi: 10.1016/j.otsr.2009.04.005.

[10] J. Michael Johnson and M. R. Mahfouz, "Cartilage loss patterns within femorotibial contact regions during deep knee bend," *Journal of Biomechanics*, vol. 49, no. 9, pp. 1794–1801, 2016, doi: 10.1016/j.jbiomech.2016.04.011.

[11] X. Paredes-Carnero, A. B. Fernández-Cortiñas, J. Escobar, J. M. Galdo, and J. G. Babé, "Management of severe valgus knee by total unconstrained arthroplasty: A comparative study with long-term follow-up," *Revista Española de Cirugía Ortopédica y Traumatología (English Edition)*, vol. 61, no. 4, pp. 240–248, 2017, doi: 10.1016/j.recote.2017.06.007.

[12] S. Donell, "Patellar tracking in primary total knee arthroplasty," *EFORT Open Reviews*, vol. 3, no. 4, pp. 106–113, 2018, doi: 10.1302/2058-5241.3.170036.

[13] J. Sun *et al.*, "Finite element analysis of the valgus knee joint of an obese child," *BioMedical Engineering Online*, vol. 15, no. s2, pp. 309–321, 2016, doi: 10.1186/s12938-016-0253-3.

[14] N. A. Z. Abidin, M. Rafiq Abdul Kadir, and M. H. Ramlee, "Three Dimensional Finite Element Modelling and Analysis of Human Knee Joint-Model Verification," *Journal of Physics: Conference Series*, vol. 1372, no. 1, 2019, doi: 10.1088/1742-6596/1372/1/012068.

[15] A. Kiapour, A. M. Kiapour, V. Kaul, C. E. Quatman, S. C. Wordeman, and T. E. Hewett, "Finite element model of the knee for investigation of injury

mechanisms: Development and validation," *Journal of Biomechanical Engineering*, vol. 136, no. 1, pp. 1–14, 2014, doi: 10.1115/1.4025692.

[16] M. T. Student, "DESIGN AND STRUCTURAL ANALYSYS OF KNEE JOINT USING," vol. 5, no. 10, pp. 19–30, 2020.

[17] S. Metan, G. C. Mohankumar, and P. Krishna, "FEM an Effective Tool to Analyse the Knee Joint Muscles during Flexion," *American Journal of Biomedical Engineering*, vol. 6, no. 2, pp. 43–52, 2016, doi: 10.5923/j.ajbe.20160602.01.

[18] V. Deshmukh, S. Bhand, M. Dangat, M. Urit, and R. Raskar, "A Review on Biomechanics of Knee Joint," *International Research Journal of Engineering and Technology*, pp. 1035–1038, 2020.

[19] S. Koo and T. P. Andriacchi, "The knee joint center of rotation is predominantly on the lateral side during normal walking," *Journal of Biomechanics*, vol. 41, no. 6, pp. 1269–1273, 2008, doi: 10.1016/j.jbiomech.2008.01.013.

[20] J. F. Abulhasan and M. J. Grey, "Anatomy and physiology of knee stability," *Journal of Functional Morphology and Kinesiology*, vol. 2, no. 4, 2017, doi: 10.3390/jfmk2040034.

[21] S. Affatato, *Biomechanics of the knee*. Woodhead Publishing Limited, 2015. doi: 10.1533/9781782420385.1.17.

[22] M. Biščević, M. Hebibović, and D. Smrke, "Variations of femoral condyle shape," *Collegium Antropologicum*, vol. 29, no. 2, pp. 409–414, 2005.

[23] M. A. Cacko and J. D. Keener, *Total Knee Arthroplasty*. 2017. doi: 10.1016/B978-0-323-28683-1.00072-2.

[24] S. L. Y. Woo, S. D. Abramowitch, R. Kilger, and R. Liang, "Biomechanics of knee ligaments: Injury, healing, and repair," *Journal of Biomechanics*, vol. 39, no. 1, pp. 1–20, 2006, doi: 10.1016/j.jbiomech.2004.10.025.

[25] J. R. Robinson, A. M. J. Bull, R. R. D. W. Thomas, and A. A. Amis, "The role of the medial collateral ligament and posteromedial capsule in controlling knee

laxity," *American Journal of Sports Medicine*, vol. 34, no. 11, pp. 1815–1823, 2006, doi: 10.1177/0363546506289433.

[26] H. H. Rachmat, D. Janssen, W. J. Zevenbergen, G. J. Verkerke, R. L. Diercks, and N. Verdonschot, "Generating finite element models of the knee: How accurately can we determine ligament attachment sites from MRI scans?," *Medical Engineering and Physics*, vol. 36, no. 6, pp. 701–707, 2014, doi: 10.1016/j.medengphy.2014.02.016.

[27] A. J. Goff and M. R. Elkins, "Knee osteoarthritis," *Journal of Physiotherapy*, vol. 67, no. 4, pp. 240–241, 2021, doi: 10.1016/j.jphys.2021.08.009.

[28] K. Wada, A. Price, K. Gromov, S. Lustig, and A. Troelsen, "Clinical outcome of bi-unicompartmental knee arthroplasty for both medial and lateral femorotibial arthritis: a systematic review—is there proof of concept?," *Archives of Orthopaedic and Trauma Surgery*, vol. 140, no. 10, pp. 1503–1513, 2020, doi: 10.1007/s00402-020-03492-6.

[29] D. Nikolopoulos, I. Michos, G. Safos, and P. Safos, "Current surgical strategies for total arthroplasty in valgus knee," *World Journal of Orthopedics*, vol. 6, no. 6, pp. 469–482, 2015, doi: 10.5312/wjo.v6.i6.469.

[30] M. Hussain *et al.*, "Ultra-high-molecular-weight-polyethylene (UHMWPE) as a promising polymer material for biomedical applications: A concise review," *Polymers*, vol. 12, no. 2, pp. 1–27, 2020, doi: 10.3390/polym12020323.

[31] R. J. Napier *et al.*, "A prospective evaluation of a largely cementless total knee arthroplasty cohort without patellar resurfacing: 10-year outcomes and survivorship," *BMC Musculoskeletal Disorders*, vol. 19, no. 1, pp. 1–9, 2018, doi: 10.1186/s12891-018-2128-1.

[32] K. Kamada *et al.*, "Mobile Bearing Total Knee Arthroplasty for Valgus Knee Osteoarthritis with Permanent Patellar Dislocation: A Case Report and Review

of the Literature," *Case Reports in Orthopedics*, vol. 2017, no. d, pp. 1–5, 2017, doi: 10.1155/2017/1230412.

[33] N. R. Klem *et al.*, "What influences patient satisfaction after total knee replacement? A qualitative long-term follow-up study," *BMJ Open*, vol. 11, no. 11, Nov. 2021, doi: 10.1136/bmjopen-2021-050385.

[34] P. Aglietti, A. Baldini, R. Buzzi, and P. F. Indelli, "Patella resurfacing in total knee replacement: Functional evaluation and complications," *Knee Surgery, Sports Traumatology, Arthroscopy*, vol. 9, no. SUPPL. 1, pp. 27–33, 2001, doi: 10.1007/s001670000160.

[35] A. M. Merican, K. M. Ghosh, F. Iranpour, D. J. Deehan, and A. A. Amis, "The effect of femoral component rotation on the kinematics of the tibiofemoral and patellofemoral joints after total knee arthroplasty," *Knee Surgery, Sports Traumatology, Arthroscopy*, vol. 19, no. 9, pp. 1479–1487, 2011, doi: 10.1007/s00167-011-1499-8.

[36] H. J. Meijerink *et al.*, "The trochlea is medialized by total knee arthroplasty: An intraoperative assessment in 61 patients," *Acta Orthopaedica*, vol. 78, no. 1, pp. 123–127, 2007, doi: 10.1080/17453670610013529.

[37] C. Becher *et al.*, "Posterior stabilized TKA reduce patellofemoral contact pressure compared with cruciate retaining TKA in vitro," *Knee Surgery, Sports Traumatology, Arthroscopy*, vol. 17, no. 10, pp. 1159–1165, 2009, doi: 10.1007/s00167-009-0768-2.

[38] M. Woiczinski *et al.*, "TKA design-integrated trochlea groove rotation reduces patellofemoral pressure," *Knee Surgery, Sports Traumatology, Arthroscopy*, vol. 27, no. 5, pp. 1680–1692, 2019, doi: 10.1007/s00167-018-5324-5.

[39] A. Keshmiri, G. Maderbacher, A. Benditz, W. Müller, J. Grifka, and B. Craiovan, "No difference in patellar kinematics between fixed-bearing cruciate-retaining and cruciate-substituting total knee arthroplasty: a cadaveric investigation,"

International Orthopaedics, vol. 40, no. 4, pp. 731–735, 2016, doi: 10.1007/s00264-015-3041-y.

[40] C. Planckaert, G. Larose, P. Ranger, M. Lacelle, A. Fuentes, and N. Hagemeister, "Total knee arthroplasty with unexplained pain: new insights from kinematics," *Archives of Orthopaedic and Trauma Surgery*, vol. 138, no. 4, pp. 553–561, 2018, doi: 10.1007/s00402-018-2873-5.

[41] T. Ingrassia, L. Nalbone, V. Nigrelli, D. Tumino, and V. Ricotta, "Finite element analysis of two total knee joint prostheses," *International Journal on Interactive Design and Manufacturing*, vol. 7, no. 2, pp. 91–101, 2013, doi: 10.1007/s12008-012-0167-7.

[42] K. Islam, K. Duke, T. Mustafy, S. M. Adeeb, J. L. Ronsky, and M. El-Rich, "A geometric approach to study the contact mechanisms in the patellofemoral joint of normal versus patellofemoral pain syndrome subjects," *Computer Methods in Biomechanics and Biomedical Engineering*, vol. 18, no. 4, pp. 391–400, 2015, doi: 10.1080/10255842.2013.803082.

[43] A. Mestar, S. Zahaf, N. Zina, and A. Boutaous, "Development and validation of a numerical model for the mechanical behavior of knee prosthesis analyzed by the finite elements method," *Journal of Biomimetics, Biomaterials and Biomedical Engineering*, vol. 37, pp. 12–42, 2018, doi: 10.4028/www.scientific.net/JBBBE.37.12.

[44] J. Wang, Y. Yang, D. Guo, S. Wang, L. Fu, and Y. Li, "The effect of patellar tendon release on the characteristics of patellofemoral joint squat movement: A simulation analysis," *Applied Sciences (Switzerland)*, vol. 9, no. 20, 2019, doi: 10.3390/app9204301.

[45] D. Kaiser, L. Trummler, T. Götschi, F. W. A. Waibel, J. G. Snedeker, and S. F. Fucentese, "The quantitative influence of current treatment options on patellofemoral stability in patients with trochlear dysplasia and symptomatic

patellofemoral instability - a finite element simulation," *Clinical Biomechanics*, vol. 84, Apr. 2021, doi: 10.1016/j.clinbiomech.2021.105340.

[46] T. Daniela, C. Marius, and T. D. Nicolae, "Modeling and finite element analysis of the human knee joint affected by osteoarthritis," *Key Engineering Materials*, vol. 601, pp. 147–150, 2014, doi: 10.4028/www.scientific.net/KEM.601.147.

[47] K. S. Halonen, M. E. Mononen, J. Töyräs, H. Kröger, A. Joukainen, and R. K. Korhonen, "Optimal graft stiffness and pre-strain restore normal joint motion and cartilage responses in ACL reconstructed knee," *Journal of Biomechanics*, vol. 49, no. 13, pp. 2566–2576, 2016, doi: 10.1016/j.jbiomech.2016.05.002.

[48] G. A. Orozco, P. Tanska, M. E. Mononen, K. S. Halonen, and R. K. Korhonen, "The effect of constitutive representations and structural constituents of ligaments on knee joint mechanics," *Scientific Reports*, vol. 8, no. 1, pp. 1–15, 2018, doi: 10.1038/s41598-018-20739-w.

[49] N. A. Watson, K. R. Duchman, N. M. Grosland, and M. J. Bollier, "Finite Element Analysis of Patella Alta," *The Iowa orthopaedic journal*, vol. 37, no. 319, pp. 101–108, 2017.

[50] Y. Dong, Z. Zhang, W. Dong, G. Hu, B. Wang, and Z. Mou, "An optimization method for implantation parameters of individualized TKA tibial prosthesis based on finite element analysis and orthogonal experimental design," *BMC Musculoskeletal Disorders*, vol. 21, no. 1, Mar. 2020, doi: 10.1186/s12891-020-3189-5.

[51] C. Belvedere, F. Catani, A. Ensini, J. L. Moctezuma De La Barrera, and A. Leardini, "Patellar tracking during total knee arthroplasty: An in vitro feasibility study," *Knee Surgery, Sports Traumatology, Arthroscopy*, vol. 15, no. 8, pp. 985–993, Aug. 2007, doi: 10.1007/s00167-007-0320-1.

[52] F. Galbusera *et al.*, "Material models and properties in the finite element analysis of knee ligaments: A literature review," *Frontiers in Bioengineering and*

Biotechnology, vol. 2, no. NOV. Frontiers Media S.A., 2014. doi: 10.3389/fbioe.2014.00054.

[53] A. Kiapour, A. M. Kiapour, V. Kaul, C. E. Quatman, S. C. Wordeman, and T. E. Hewett, "Finite element model of the knee for investigation of injury mechanisms: Development and validation," *Journal of Biomechanical Engineering*, vol. 136, no. 1, 2014, doi: 10.1115/1.4025692.

[54] L. Zabawa, K. Li, and S. Chmell, "Patient dissatisfaction following total knee arthroplasty: external validation of a new prediction model," *European Journal of Orthopaedic Surgery and Traumatology*, vol. 29, no. 4, pp. 861–867, May 2019, doi: 10.1007/s00590-019-02375-w.

[55] S. Farrokhi, J. H. Keyak, and C. M. Powers, "Individuals with patellofemoral pain exhibit greater patellofemoral joint stress: A finite element analysis study," *Osteoarthritis and Cartilage*, vol. 19, no. 3, pp. 287–294, Mar. 2011, doi: 10.1016/j.joca.2010.12.001.